EFFECTS OF RETROFITTING APPLICATIONS ON REINFORCED CONCRETE BRIDGES

Introduction:

Reinforced concrete bridges constructed prior to 1971 have been designed with little or no ductility considerations and are particularly vulnerable to damage when exposed to a moderate earthquakes. Various retrofit applications have been developed for improving the strength and ductility of bridges or bridge components. The objective of this research is to evaluate the effects of different retrofit applications on the global response of short-spanned reinforced concrete bridges.

Research Approach:

A three-dimensional nonlinear finite-element model of the Dry Wash Bridge was developed and the results were used as the baseline in the parametric studies. A nonlinear modal pushover procedure was employed to perform the analyses in the longitudinal and transverse direction of the bridge. Retrofitting methods addressed in this study include steel jacketing of columns, foundation, and abutment retrofit. Modeling element characterizations that vary with the associated retrofit applications are taken as parameters in the sensitivity study. The corresponding parameters representing structural elements include linear foundation springs, nonlinear abutment springs, and various column-jacketing plans. Results from varying parameters were compared with the baseline to conduct sensitivity study.

Conclusions and Recommendations:

Results show that the force demands are changed as much as 100% of the baseline in the presence of varying foundation and abutment stiffness. However, the variation in the associated displacement capacity is within a range of 20% or less. Bridges supported on softer foundations can tolerate larger displacements, and induce less force input to the superstructure. However, the ductility may be decreased due to the postpone of yielding of the structure. Analyses should be performed to estimate the "trade-off" of ductility and force demand reduction due to foundation stiffness change. For the Dry Wash Bridge a flexible foundation connection is recommended. Softer abutments do not produce ductile response of the bridge, but decrease the force demand on the structure.

Column steel jacketing presents the best capability to improve the bridge ductility. By comparing results from the eighteen cases of different column retrofit combinations, it is concluded that the middle columns and columns with shorter effective height are more critical in improving the bridge longitudinal ductility. In the transverse direction, priority should be given to columns with shorter effective height. Analytical research should further be carried out to better understand the performance of a specific bridge and locate the vulnerable columns prior to the implementation of a specific retrofitting plan.

Project Personnel:

Rafik Itani
Principal Investigator
Washington State University
Dept. of Civil & Environ. Engineering
PO Box 642910
101 Sloan Hall
Pullman, Washington 99164-2910

Xin Liao
Graduate Research Assistant
Washington State University
Dept. of Civil & Environ. Engineering
PO Box 642910
101 Sloan Hall
Pullman, Washington 99164-2910

Research Report

Research Project T 2696, Task 02
Retrofitting Applications on Bridges

EFFECTS OF RETROFITTING APPLICATIONS ON REINFORCED CONCRETE BRIDGES

by

Rafik Itani and Xin Liao
Department of Civil and Environmental Engineering
Washington State University
Pullman, WA 99163

Washington State Transportation Center (TRAC)
Civil and Environmental Engineering; Sloan Hall, Room 101
Washington State University
Pullman, Washington 99164-2910

Prepared for
Washington State Transportation Commission
Department of Transportation
and in cooperation with
U.S. Department of Transportation
Federal Highway Administration

August, 2003

1. REPORT NO.	2. GOVERNMENT ACCESSION NO.	3. RECIPIENT'S CATALOG NO.
WA-RD 570.1		

4. TITLE AND SUBTITLE	5. REPORT DATE
EFFECTS OF RETROFITTING APPLICATIONS ON REINFORCED CONCRETE BRIDGE	August, 2003
	6. PERFORMING ORGANIZATION CODE
7. AUTHOR(S)	8. PERFORMING ORGANIZATION REPORT NO.
Itani, Rafik	
9. PERFORMING ORGANIZATION NAME AND ADDRESS	10. WORK UNIT NO.
Washington State Transportation Center (TRAC) Civil and Environmental Engineering; Sloan Hall, Room 101 Washington State University Pullman, Washington 99164-2910	11. CONTRACT OR GRANT NO. T2696-02
12. SPONSORING AGENCY NAME AND ADDRESS	13. TYPE OF REPORT AND PERIOD COVERED
Research Office Washington State Department of Transportation Transportation Building, MS 7370 Olympia, Washington 98504-7370	Research Report
	14. SPONSORING AGENCY CODE

15. SUPPLEMENTARY NOTES

16. ABSTRACT

The objective of this research is to evaluate the effects of different retrofit applications on the global response of short-spanned reinforced concrete bridges. The global responses investigated include structural displacement and ductility. Modeling element characterizations that vary with the associated retrofit applications are taken as parameters in the sensitivity study. Retrofitting methods addressed in this study include steel jacketing of columns, foundation, and abutment retrofit. The corresponding parameters representing structural elements include linear foundation springs, nonlinear abutment springs, and various column-jacketing plans. A three-dimensional nonlinear finite-element model of the Dry Wash Bridge was developed and the results were used as the baseline in the parametric studies. A nonlinear modal pushover procedure was employed to perform the analyses in the longitudinal and transverse direction of the bridge. Results were analyzed by conducting parametric study to evaluate the effects of different retrofit schemes on the bridge global behavior.

17. KEY WORDS	18. DISTRIBUTION STATEMENT
Key words: Reinforced concrete bridge retrofitting, parametric study, column steel jacketing, foundation spring, abutment spring, structure ductility	No restrictions. This document is available to the public through the National Technical Information Service, Springfield, VA 22616

19. SECURITY CLASSIF. (of this report)	20. SECURITY CLASSIF. (of this page)	21. NO. OF PAGES	22. PRICE
None	None		

DISCLAIMER

The contents of this report reflect the views of the authors, who are responsible for the facts and the accuracy of the data presented herein. The contents do not necessarily reflect the official views or policies of the Washington State Transportation Commission, Department of Transportation, or the Federal Highway Administration. This report does not constitute a standard, specification, or regulation.

TABLE OF CONTENTS

LIST OF FIGURES

LIST OF TABLES

EXECUTIVE SUMMARY

Reinforced concrete bridges constructed prior to 1971 have been designed with little or no ductility considerations and are particularly vulnerable to damage when exposed to a moderate earthquakes. Over the past several years, various retrofit applications have been developed for improving the strength and ductility of bridges or bridge components to ensure their safety and compliance with code requirements. Question, however, remains regarding the need to evaluate the effect of selective retrofitting applications on the global response of a bridge.

The objective of this research is to evaluate the effects of different retrofit applications on the global response of short-spanned reinforced concrete bridges. The global responses investigated include structural displacement and ductility. Modeling element characterizations that vary with the associated retrofit applications are taken as parameters in the sensitivity study. Retrofitting methods addressed in this study include steel jacketing of columns, foundation, and abutment retrofit. The corresponding parameters representing structural elements include linear foundation springs, nonlinear abutment springs, and various column-jacketing plans. A three-dimensional nonlinear finite-element model of the Dry Wash Bridge was developed and the results were used as the baseline in the parametric studies. A nonlinear modal pushover procedure was employed to perform the analyses in the longitudinal and transverse direction of the bridge.

Results show that the force demands are changed as much as 100% of the baseline in the presence of varying foundation and abutment stiffness. However, the variation in the associated displacement capacity is within a range of 20% or less. Bridges supported on softer foundations can tolerate larger displacements, and induce less force input to the superstructure. However, the ductility may be decreased due to the postpone of yielding of the structure. Analyses should be performed to estimate the "trade-off" of ductility and force demand reduction due to foundation stiffness change. For the Dry Wash Bridge a flexible foundation connection is recommended. Softer abutments do not produce ductile response of the bridge, but decrease the force demand on the structure.

Column steel jacketing presents the best capability to improve the bridge ductility. By comparing results from the eighteen cases of different column retrofit combinations, it is concluded that the middle columns and columns with shorter effective height are more critical in improving the bridge longitudinal ductility. In the

transverse direction, priority should be given to columns with shorter effective height. Analytical research should further be carried out to better understand the performance of a specific bridge and locate the vulnerable columns prior to the implementation of a specific retrofitting plan.

INTRODUCTION

BACKGROUND

It has been observed that most of the bridges damaged in earthquakes were constructed before 1971 and had little or no design consideration to seismic resistance. The vulnerability of pre-1971 bridges was especially evident in the 1989 Loma Prieta earthquake, the 1994 Northridge earthquake, and the 2001 Nisqually earthquake. Since the 1971 San Fernando earthquake in California, the standards for earthquake design have been strengthened considerably, and bridge structural behavior has been more accurately evaluated. Since then, structural ductility, a crucial element for the survival of bridges under severe earthquakes, has become a key consideration in structural analysis and design. In addition, capacity design has been implemented, thus seismic performance of bridges has been greatly improved.

However, bridges that were constructed prior to 1971 are still in use and play important roles in our transportation systems, which may be susceptible to failure due to their structural deficiencies. To ensure safety and performance of these bridges, a seismic retrofit and strengthening program has been one of the major efforts of the Washington Department of Transportation and the Federal Highway Administration, aiming at improving seismic performance of older bridges. Various retrofit and strengthening techniques have been developed and implemented. Furthermore, experimental and analytical researches have been conducted to verify the effectiveness of those techniques. Retrofitting methods such as restrainers and column jacketing have proven to be effective in recent earthquakes. Techniques to retrofit other bridge members have also been developed such as soil anchors, footing retrofit involving increased plan dimension and reinforced overlay, construction of link beams, and system isolation and damping device.

While most of the studies were aimed at investigating the effectiveness of a particular retrofit technique, few studies have been conducted to evaluate the global bridge structural system behavior after various retrofit techniques are implemented. In the State of Washington, a typical retrofitting scheme for old reinforced concrete bridges is to jacket every columns of the bridge. This may not be necessary due to the expensive nature of retrofitting. The goal of seismic retrofit is to minimize the likelihood of structural failure while meeting certain performance requirements. This allows engineers to design repair strategies based on performance needs. As a consequence, some level of damage may be acceptable during a design-level earthquake. The

California Department of Transportation (Caltrans) has required that bridge retrofits provide survival limit-state protection at seismic intensities appropriate for new bridges. This makes possible the proposition of efficient and effective strengthening measures with optimized retrofitting schemes, and the adoption of the plan that is the most economical for the acceptable damage level.

OBJECTIVE OF THE RESEARCH

The purpose of this research is to evaluate the effects of retrofit applications on the global performance of typical short-spanned reinforced concrete bridges. A three-dimensional nonlinear finite-element model of a reinforced concrete bridge, the Dry Wash Bridge, was developed to determine the inelastic response by performing nonlinear pushover analysis. Modal pushover analyses were carried out in both longitudinal and transverse directions. Detailed data of performance were collected and interpreted to use as a baseline in a parametric study. Because retrofitting applications for different bridge components can change the characterizations of modeling elements, the properties of these elements were taken as varying parameters in the sensitivity study. Retrofitting applications addressed include foundation retrofit, abutment retrofit and column steel jacketing. Parametric analyses were performed to evaluate the effects and sensitivity of the global performance of the bridge to the applications of various local retrofitting. Different column retrofitting plans are compared to estimate their efficiency in enhancing the structure global ductility.

LITERATURE REVIEW

In the United States, 60 percent of all bridges were constructed before 1970 without adequate consideration to seismic resistance. These bridges were obviously vulnerable in recent earthquakes. In the Northridge quake, 1994, six bridges failed and four bridges were severely damaged. The failure of those bridges was primarily due to the failure of the supporting columns that had been designed and constructed before 1971 (Cooper, et al. 1994). On February 28th, 2001, the 6.8-magnitude Nisqually earthquake damaged 78 bridges. A big majority of these bridges (80%) were built before 1970 (Ranf et al. 2001).

In this chapter, a comprehensive elaboration of bridge damages is detailed, and corresponding retrofitting technique of different bridge components and their performance are illustrated. A review of researches related to the global performance of bridge retrofit and strengthening techniques is presented.

BRIDGE DAMAGES AND CORRESPONDING RETROFIT METHODS

In reviewing bridge damages caused by recent earthquakes, three basic design deficiencies can be identified: seismic deflections were seriously underestimated; low seismic force levels were adopted; inelastic structural actions and associated concepts of ductility were not considered. All of the structural deficiencies tend to be a direct consequence of the elastic design philosophy, which was almost uniformly adopted for seismic design of bridges prior to 1970 (Priestley et al. 1996).

Superstructure and Cap Beam

The most common reasons causing superstructure failure is unseating at movement joints due to the large inelastic displacements shown in Figure 1. If bridges were built on soft or liquefiable soils, the displacement may be even amplified when an earthquake hits. In the 1971 San Fernando earthquake, most of the bridge failures were caused by the loss of supports at bearing seats and/or expansion joints.

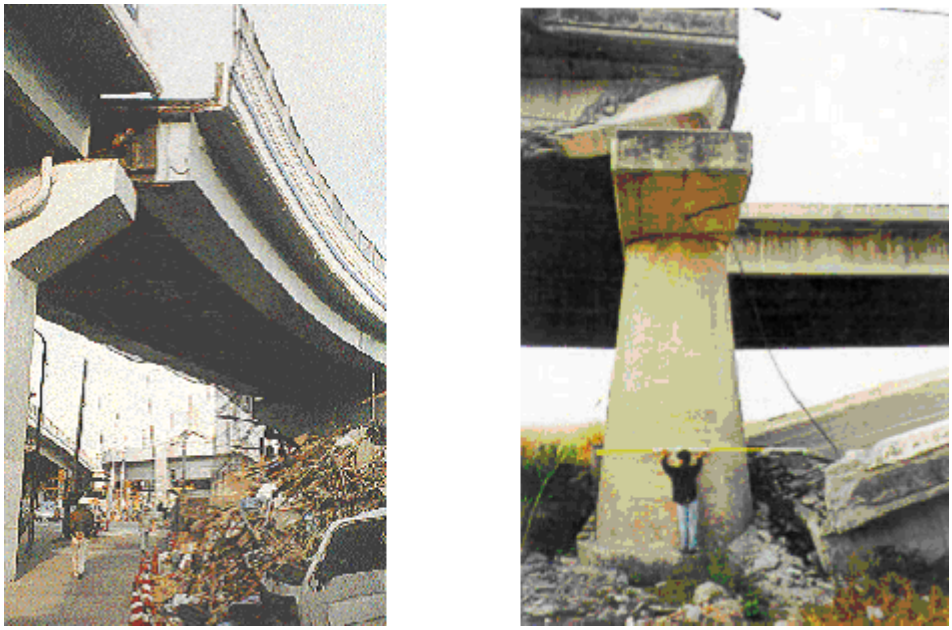

Figure 1 Bridge superstructure failures: (left) superstructure lateral offsets in 95' Kobe earthquake, Japan (Ghasemi, et al., 1994); (right) fallen Beam due to superstructure movement, Wushi Bridge, Taiwan. (Hsu, Y. T. et al., 2000)

To deal with this problem, restrainers are installed to strengthen superstructure of bridges, such as longitudinal joint restrainers, transverse-bearing restrainers, and vertical restrainers. These restrainers can help increase displacement capacity by tying the various parts of a bridge together. In the State of California, installing restrainers is in the first phase of retrofitting effort, and design method was proposed by Priestley et. al (1996).

Cap beams usually failed in flexural strength and shear strength, especially in the outrigger bent caps. Insufficient anchorage of cap beam reinforcement into the end region is another deficiency widely observed in many older multicolumn bents.

The cost of cap beams retrofit is high besides the fact that the construction can be complicated. One method to reduce the cap beam seismic forces is to launch a link beam at proper height to redistribute the load demand. If flexural strength of cap beam is to be enhanced, reinforced concrete bolsters can be added to the sides of existing cap beams after roughening the interface. The new and old concrete members should be connected by dowels, preferably passing through the existing cap beam. Thus, the section of the integral cap beam is enlarged, and shear strength can be increased.

Bridge columns

Figure 2 shows the spalling and crushing of column in Northridge earthquake, 1994. Column failure is mainly due to deficiencies in flexural strength and ductility, or shear strength. Two failure modes of reinforced concrete piers were commonly observed in recent earthquakes. The first category is flexural failure and lack of flexural ductility, which primarily occur in plastic hinge regions. This may result from a deficient detail that insufficient splicing length of the longitudinal bars was provided at the bottom of the columns.

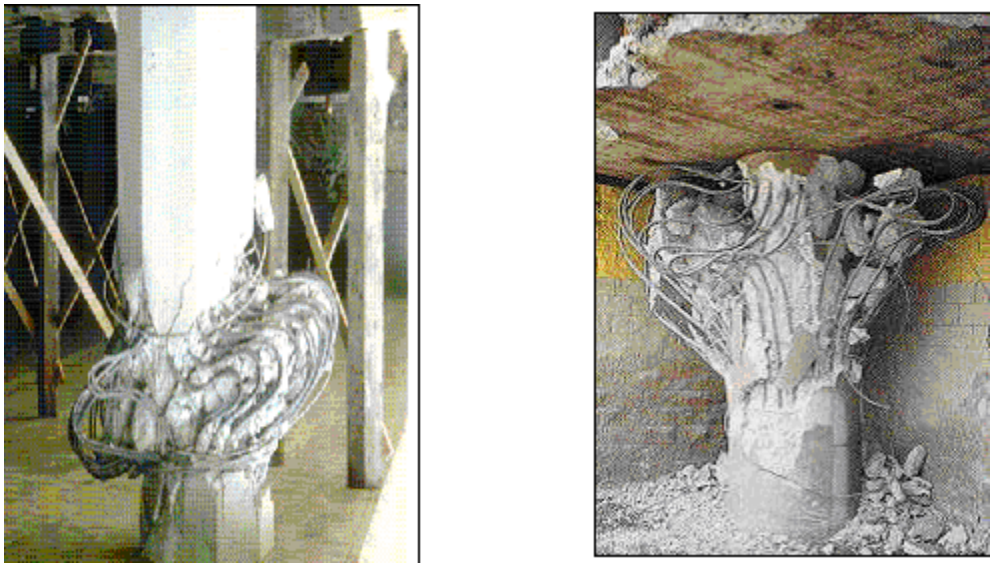

Figure 2 Column failures in 94' Northridge quake, (a) spalling at column end; (b) crushed column due to insufficient concrete-core confinement. (Cooper, et al., 1994)

The second category of column failure is shear failure. Shear failures are brittle and lead to a quick degradation of the lateral strength of a pier, which may be more catastrophic than flexural failure. Short columns with conventional transverse reinforcement details are particularly vulnerable to shear failure. In these old bridge columns, it was typical to use No. 3 or No. 4 hoops spaced at 300mm (12in.) on center regardless of column cross-sectional dimensions and only lapped the ends in the cover concrete bars (Daudey and Filiatrault, 2000). This has been proved an insufficient amount of transverse reinforcement. Better confinement was necessary to prevent crushing rapidly extending into the core, so that to help stop the buckle of the longitudinal reinforcement so as to avoid rapid strength degradation.

Column jacketing is the most common retrofit method to provide better confinement to as-built columns. Among various types of jackets, steel jackets have been the most widely implemented. In standardized column retrofit procedures proposed by

the Caltran, steel jackets are typically employed (Caltrans, 1999). The procedure was originally developed for circular columns that jacketed with thin steel plates or half shells site-welded up to form a continuous tube as shown in Figure 3. At the end of the jacket, a 50mm (2in.) gap is necessary between the supporting member and the jacket. The gap is grouted with cement grout. This is to avoid increase in stiffness at plastic hinge region to attract greater internal forces to transfer to footing or cap beams.

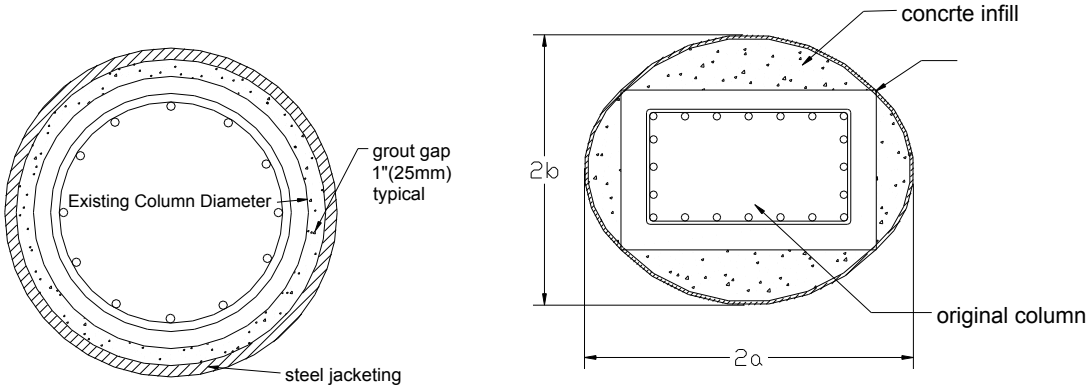

(a) Circular column (b) Rectangular column

Figure 3 Confinement of columns by steel jacketing (adopted from Priestley, 1996)

Rectangular columns usually employ elliptical jackets as shown in Figure 3(b). A steel jacket of rectangular shape on shear critical concrete columns are a good alternative if special details are applied per the study of Abouraha et al. (1999) shown in Figure 4. Other improved retrofit techniques also exist such as steel jackets with adhesive anchor bolts, and steel jacket with through rods and welding of the lap splice.

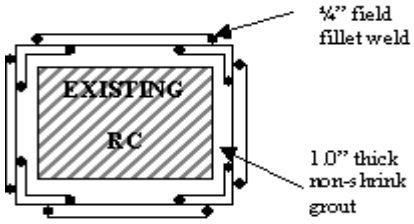

Figure 4 Steel jacket of a column in a rectangular shape (Aboutaha, et al. ,1999)

Because steel jackets have the possibility of deterioration of the bond between jackets and the concrete due to long-term exposure to the weather, concrete jackets are utilized and can relatively easily achieve an enhanced confinement by placing close-spaced hoops or a spiral of small pitch. Other materials, such as fiberglass plate previously used in building structures, are applied as jackets on bridge columns as well.

Substructure

Substructure failures include footing and abutment failures. Footing usually fails due to deficiencies in footing strength, anchorage of column rebar, and overturning resistance. In early design codes, bridges were primarily designed for gravity loads; little or no lateral forces from earthquake were considered. As a result, the foundations in older bridges primarily designed for gravity loads were undersized, and vulnerable to overturning. The Caltran has developed general procedures for designing foundation retrofits. Flexural strength, shear strength and overturning are three aspects to be checked in the procedure. If actions to increase overturning resistance are taken, such as enlarging the size of the foundation and placing soil anchors, the negative moment demand on the top of the footing is increased. So an overlay of reinforced concrete doweled to the existing footing is necessarily to prevent failure to occur due to flexural failure, and also increase the shear resistance.

The rocking of footings may be considered as a form of seismic isolation, which is advantageous. It can be permitted if superstructure is continuous over the full length and the abutments are strong. Damping devices should be placed between the superstructure and abutments to limit the rocking displacement.

When the rocking is unacceptable, some remedial actions may be applied to increase footing overturning capacity and to enhance the connection of the footing to the piles. Methods include placing soil anchors and increasing footing plan dimensions and placing additional piles.

Reports of foundation damage were not very common in bridge, except where caused by soil liquefaction or ground sliding. However, footing retrofit can be potentially the most expensive comparing with other bridge members. Consequently, design of footing retrofit requires careful considerations.

In recent earthquakes slumping of abutment fill and rotation of abutments were found widespread, which is related to soft soils and the effective engagement of abutment backwall on longitudinal direction and wingwall on transverse direction.

Similar retrofit methods can be applied to abutments to increase the locking of movement joints, such as providing cable or restrainers between the elements. If locking movement joints is not desirable, the effective seating length of the movement joint should be extended by corbels or brackets added to the sides of abutments.

Joints Retrofitting

Unlike building structures, knee joints and vertical tee joints are more commonly seen than beam-column joints that are full intersections of columns and beams. Joints behavior in bridges may be very complicated under seismic loading for a retrofit technique to be addressed.

Typically, a number of options are available for joints repair, such as joint prestressing, jacketing, and joint replacement. Joint force reduction is by implementing link members in the bent to redistribute the loading. Link beams can reduce forces in joints as well as in cap beams, which improves the whole structure internal force distribution.

Joint retrofitting method is not addressed in this study, because the behavior of joints is very complicated and varies in different bridges. It is assumed that all joints of the bridge have sufficient strength and performance capacity in this research.

Link Beams

Link beams can be located at the column mid-height or above the footing, with different purposes to distribute the internal forces and change the structure stiffness. Link beam can be designed to force the plastic hinges to form into the column above or below the hinge, or even form at the ends of the link beams, so as to protect the columns from inelastic actions to occur at the mid-height. By varying the location of the link beams, force reduction can be achieved for weak elements. It is advantageous that during construction of link beams the traffic is not necessarily disrupted.

In this research, the effect of link beams is not discussed due to its high variability for different retrofit purpose.

PERFORMANCE EVALUATION

Various researches have been conducted to evaluate the performance of retrofitting methodologies. The following results are from studies related to the present research.

Steel Jacketed Column Performance

Prestley et al. (1994) conducted a program of 14 large-scale column tests involving "as-built" and steel-jacketed columns. In the experiments, circular columns were retrofitted with steel jacket, filled in cement grout; and rectangular columns employed elliptical steel jackets. In the "as-built" columns, shear deformation was predominated,

but in jacketed columns it was changed to flexural predominated. As a result, all the "as-built" columns failed brittle in shear, or because of low flexural ductility. Jacketed columns exhibited extremely stable lateral force-displacement hysteretic response. The flexural over-strength of strengthened columns was averagely 29 percent more than the calculated strength based on an extreme compression strain of 0.005, including effects of confinement and strain hardening. Elastic stiffness of the columns was on average increased 30 percent for circular columns, 64 percent for rectangular columns. The displacement ductility capacity was tested to be greater than or equal to $\mu_{\Delta} = 8$, and with drift angles of 4 percent or greater.

Daudey and Filiatrault (2000) conducted both experimental and numerical analysis for steel jacketed reinforced concrete bridge piers with complex cross-sectional geometries and lap-splices in plastic hinge region. The overall behavior proved to be very good. The tests indicated that the gap size of 50mm (2 inches) between the bottom of jacket and the top of the footing is adequate. This distance is effective to prevent stress concentration in the longitudinal reinforcement and avoid premature bar failure in tension at large inelastic displacement. The experiment also indicated that the geometry of the steel jacket does not influence on the efficiency of the reinforcement. Stable hinging occurred in the gap, where inelastic deformations sustained without significant strength loss. The displacement ductility reached 6.0, before sliding of longitudinal bars took place. The research also verified the prediction of the plastic hinge length, L_p, of a reinforced concrete pier retrofitted with steel jackets by Priestley (1996). It is Equation 4-11.

Foundation Retrofitting Performance

To investigate bridge foundation retrofitting methodology, McLean and Marsh (1999) conducted experiments on footing retrofit by adding a reinforced overlay on existing footings. The technique provided an effective retrofit for the as-built footings. The "as built" specimen failed due to the inadequacy of joint shear strength, which was a brittle failure with little energy dissipation. Adding a reinforced overlay did not only increase shear resistance, but also allowed to develop plastic hinging in columns and resulted in ductile response under simulated seismic loading. It was also proposed in the research that the splice length to be expanded from $20d_b$ to 35 d_b for better integrity of the splices.

It was found that with soil anchors the uplift of the specimens was negligible, and the response was ductile and specimens failed due to low-cycle fatigue fractures of

longitudinal bars under simulated cyclic loadings. Specimens with rocking resulted in uplift and rotation of footings and consumed little energy. However, the response was stable, which could allow load redistribution and cost saving if some footings can remain unretrofitted, and rocking can be acceptable in an earthquake.

Xiao, et al. (1996) also tested four bridge footings, among which one was an "as built" model and the other three were retrofitted models. It was observed that for the "as built" model, if no dependable tension capacity was provided by the piles, rocking tended to dominate the response, which resulted in an elastic behavior and diminished the damage to its minimal. If rocking was restrained, the "as built" column footing failed in shear in a brittle fashion.

Both of the above researches indicated that if allowed, rocking of footings may be beneficial to the global response of a bridge. It was recommended that special damping device to be utilized at possible rocking footings to produce more ductile response (Priestley, 1996).

Global Performance Of Bridges Affected By Bridge Components

To evaluate retrofit strategies for multi-column bridges, Cofer, McLean and Zhang (1997) conducted analysis with a modified nonlinear dynamic bridge analysis program. Column softening behavior and reduction of stiffness were considered in the research. A 2-D structural model of an actual bridge, which consisted of five columns, was used to evaluate different column retrofitting measures. Some partial retrofit strategies were applied and the performances were compared. The existing bent would fail due to the nonductile column designs. It was found that as the number of retrofitted columns in a bent increased, the ductility capacity would increase. Some partial retrofit plans could improve the seismic resistance the bridge, but could remain the unretrofitted columns in danger. A careful examination of available retrofit options was recommended as essential to ensure severe column damage not to occur in unretrofitted columns.

As explained previously, retrofitting applications on bridge abutment would change the characterizations of abutment modeling elements, which in most cases are nonlinear springs. To estimate the contribution of bridge abutments to overall bridge seismic response, Mackie and Stojadinovic (2002) utilized Probablistic Seismic Demand Analysis (PSDA) to conduct the sensitivity study. Investigated parameters included the abutment longitudinal stiffness, transverse stiffness and the participating mass. Drift ratios and displacement ductility were compared. It was concluded after the nonlinear dynamic analysis that the mass associated with the abutment is the most critical

parameter. Stiffer abutments could reduce the response, but the difference between stiffness levels was not appreciable. Global response is insensitive to the longitudinal stiffness. Transverse stiffness values affect the global response more but the sensitivity was reduced given that the participating mass dominated the response. A simplified modeling of abutments with rollers was recommended to conservatively analyze a given bridge.

The above studies were performed with nonlinear dynamic analysis methods. However, there are many uncertainties in a time-history analysis, such as the site-specific input and analytical models. Simplified quick estimates of system response can be sufficient to provide reasonable estimations of seismic demands and structure capacity. In as displacement-based design, a relationship between spectral deformation demand and structural displacement capacity is desirable. Nonlinear pushover analysis with capability of capacity spectrum is one of the best simplifications for nonlinear dynamic analysis.

Abeysinghe, et al. (2002) utilized nonlinear pushover method to determine the expected inelastic response of the Greveniotikos Bridge during a design-level earthquake. A 3-D finite-element model was set up for the bridge, which consisted of ten bents of single column bent. Parametric studies on foundation stiffness, P-Δ effect and plastic hinge properties were carried out to evaluate the effects of different assumptions made in structural modeling and analysis. As a result, different foundation stiffness did not result in significant variations in the expected inelastic displacement. The P-Δ effect during the structural deterioration was substantially negligible in the bridge. Various properties of plastic hinges and pier cross section resulted in a difference of global response, which was less than that from varying foundation stiffness, and became negligible.

The above research provided a good example by setting up a 3D modeling and generating capacity spectrum of the bridge to evaluate structure performance. In the present research, similar methodology is employed.

RESEARCH METHODOLOGY

NONLINEAR PUSHOVER PROCEDURE

It has been proven that elastic analysis procedures used in the past for the assessment of bridge behavior are insufficient due to the inability to capture the modification of bridge response when inelastic action occurs. Time-history analysis is still regarded as the most accurate method to predict structure seismic response. However, nonlinear dynamics analysis is time and cost consuming, besides the fact that it is based on uncertain site-specific input. In addition, the effort for detailed modeling and analysis may not be warranted. Nonlinear static analysis procedures have become a preferred analysis tool in evaluation of the inelastic seismic behavior of typical structures because of its low costs in both time and money.

Pushover analysis is a nonlinear static analysis that can be used to determine displacement capacity of structures, and estimate available plastic rotational capacities to ensure satisfactory seismic performance. It helps demonstrate how the structures behave by identifying modes of failure and the potential of progressive collapse.

Seismic demands in pushover analyses are estimated by lateral loads that monotonically increase at each time step during the analysis procedure. The load modes remain the same, until a prescribed displacement is reached or the structure collapses. The equivalent seismic loads can be forces as well as displacements, and the associated control methods are force and displacement control methods. There are some disadvantages of the force control method. Firstly, after inelasticity develops in the structure, it is difficult to redefine the incremental force vectors at each step of the increment analysis. Secondly, the maximum lateral force may possibly be reached and terminate the analysis prior to developing the ultimate displacement. Therefore, the displacement control method is more appropriate and is adopted in this research. A target displacement is prescribed at a monitored point, which is usually the mass center of a bridge. SAP 2000 Nonlinear (SAP, 2000) was utilized as the tool for the analyses.

RESEARCH APPROACH

The general procedure of this research consisted of the following steps. First, a three-dimensional finite element model for the Dry Wash Bridge was set up, and pushover analysis was conducted in both the longitudinal and transverse directions. Results from the pushover analysis were analyzed and taken as the baseline for further parametric study on retrofitting applications. Secondly, test cases were run to verify

modeling assumptions on abutment rotation restraints. Thirdly, parametric study was performed on varying linear foundation stiffness and nonlinear abutment stiffness. Different column retrofitting plans were also applied to the baseline model, and results for the global response were compared to estimate the influence of these strategies. Discussion was carried out based on the influence these varying parameters made on the structure ductility and force demands.

The nonlinear parameters represented in this research include the material nonlinearity, and the geometric nonlinearity (P-delta effect). The three-dimensional nonlinear finite element model represented the geometry, effective member characterization and boundary conditions. The computed plastic hinge properties were assigned to the discrete hinges on the frame elements.

The gravity loads applied include the self-weight and the utility load of the bridge. Vertical seismic actions were not considered. The pushover loading was not the simple lateral force but related to structure mode shapes. The equivalent lateral seismic load was proportional to a specified mode shape, its angular frequency and the mass tributary to a node where the force is applied. It can be calculated as in Equation 3-1 (SAP, 2000):

$$F_{ij} = d_{ij} \times \varpi_j^{\,2} \times m_i \qquad \text{(Equation 1)}$$

In equation 1, i represents the node number, and j represents the mode number. The displacement of node "i" in the "j" vibration mode with the circular frequency of $\_j$, is d_{ij}. In each direction, modes included in the loadings excited over 90% participating mass. The mass tributary to the node "i" is m_i. Accordingly, the force applied to node "i" in the "j"th vibration mode is F_{ij}. The equivalent loading was generated by SAP (2000) after the modes are specified. The controlling displacement at the monitored point was prescribed larger than the estimated possible ultimate displacement. The structure was pushed until its ultimate capacity was reached and a global failure formed.

After the pushover analysis has been performed, a static pushover curve and a capacity spectrum of the structure could be generated for each load case. The pushover curve was in the form of the displacement at the monitored point verses the base shear, which is the total force reaction on all the supports in a given global direction. The sequence of the hinge formation and the color-coded state of each hinge can be viewed graphically, on a step-by-step basis for each step of the pushover. The member forces can also be viewed on a step-by-step basis.

The capacity spectrum plots the pushover curve in the Acceleration-Displacement Response Spectrum (ADRS) format, in which both the structural capacity (pushover) curve and the demand spectra are in spectral acceleration versus spectral displacement

coordinates. The generation of ADRS follows the procedure for a single demand spectrum with variable damping defined in ATC-40 (ATC, 1996). A family of demand spectra curves, each with a different effective damping ratio, β_{eff} , can also overlay on the capacity spectrum. The different effective damping ratio, β_{eff} , is set as 0.05, 0.1, 0.15 and 0.2 by default. The performance point of the structure is the intersection of the ADRS curve and the capacity curve. Its location relative to the performance level defined by the capacity curve indicates whether the performance objective is met or not.

These results provide a good demonstration of the behavior of the bridge, and can be utilized to conduct parametric studies. The results from the different retrofitting applications were compared with the original baseline response to estimate the sensitivity and effectiveness. It is an exploration of the corresponding effects of incorporating various retrofitting methods on the structure.

PARAMETRIC ANALYSES OF RETROFIT METHODS

Modeling parameters that vary with the retrofit applications were taken as parameters in the sensitivity study. Three retrofitting aspects were chosen as parameters for the study, namely, foundation retrofit, abutment retrofit and column retrofit with steel jacketing. The corresponding parameters are linear foundation stiffness, nonlinear abutment spring stiffness, and column jacketing plans.

As elaborated in the previous chapters, retrofit application can change the properties of modeling parameters. For example, to increase the overturning resistance of a footing, the size of the footing can be enlarged and soil anchors can be applied. These applications alter the force-displacement relationship of the footing, and can be estimated as an increase of the footing spring stiffness in the bridge model. Hence, foundation stiffness was taken as one parameter to be tested in order to evaluate the effect of foundation local retrofit on the global response of the structure.

Similarly, the abutment lateral stiffness was taken as another parameter to test the sensitivity of the global response to the variation of the abutment nonlinear force-displacement characterization.

The third retrofit application studied was selective column steel jacketing plans. The main objective of steel jacketing is to enhance the column ductility by providing better confinement to the column core concrete. After steel jacketing, the column moment-rotation capacity is greatly increased, which correspondingly improve the ductility of the selective jacketed columns. Plans investigated consisted of different number of columns at different bridge bents to be retrofitted. It was assumed that

columns were jacketed over the whole length; so plastic rotation capacity at both top and bottom hinges were increased.

Results compared were structure displacement capacity and structure ductility. The maximum displacement at the monitored point was regarded as the indicator of structure displacement capacity. Performance ductility taken as the ratio of the maximum displacement over the performance displacement is used to indicate structure ductility.

MODELING OF THE BRIDGE

GLOBAL GEOMETRIC MODELING

A spine model shown in Figure 5 was employed in the modeling with line elements following the center of gravity of cross sections along the length of the bridge. Bridge bents were modeled with a frame along the bent axis. A photograph of the Dry Wash Bridge is shown in Figure 17, and the detailed description of the bridge is given in section 4.5. Line elements can behave three-dimensionally in the form of beam, column-beam elements and springs.

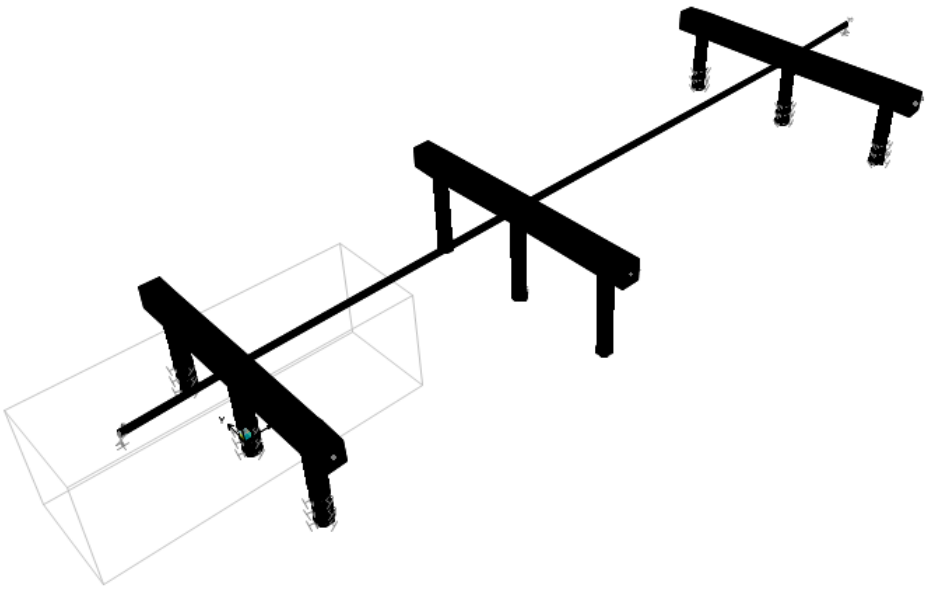

Figure 5 Spine model of Dry Wash Bridge set up by SAP 2000 Nonlinear

Superstructure of a bridge consists of a bridge deck and a support system of bents, which can be critical in an analysis process. Due to the large in-plane rigidity, the superstructure can be assumed as a rigid body for lateral loadings. The modeling objective of this research was to model the stiffness and mass distribution of superstructure and the bents. Short spanned bridges are very stiff in superstructure and can be modeled with spine beam elements that represent effective stiffness characterization. However, the spine model is not a good representation of the mass distribution. The loading in this research is proportional to the specified mode shape, the frequency and the mass tributary to the node where the lateral force is applied. So to avoid assembling of the mass in the center of the superstructure, the tributary masses of the superstructure were assigned to the nodes at the top of the columns.

The bridge investigated in this research is multi-columned at each bent, where framing action and coupling between columns can contribute to the seismic resistance in terms of stiffness, resistance capacity and axial load levels in the various frame members. In the analytical model, all of these effects were incorporated in a planar frame model along the bent axis. Effective or cracked stiffness properties should be assigned to the moment of inertia of the entire cross section about the transverse axis, I_y. The derivation of effective moment of inertia is based on the cracked section, and can be estimated to be 35% to 60% of the gross section moment of inertia. However, it is sufficient to use $I_e=0.5I_g$ which results in an effective flexural stiffness as given by Equation 2 (Priestley, 1996):

$$EI_e = \begin{cases} 0.5EI_g & \text{(reinforced concrete)} \\ 1.0EI_g & \text{(prestressed concrete)} \end{cases} \qquad \text{(Equation 2)}$$

The torsional rigidity, J, can be determined using Equation 3 (Priestley, 1996):

$$J = \frac{4A_0^2 t}{p_0} \qquad \text{(Equation 3)}$$

in which A_0 and p_0 represent respectively, the area and perimeter of the shear flow in the tubular section of wall thickness t.

Column elements are extended into cap or footing. The extension length was the tensile strain penetration length that will be detailed later. For columns, the effective member stiffness, EI_e, the effective shear stiffness, GA_{ve}, the effective axial stiffness, EA_e, should be employed. These properties were reduced from the gross-section properties in proportion to the effective flexural stiffness shown as Equation 4 (Priestley, 1996).

$$EA_e = EA_g \frac{EI_e}{EI_g}$$
$$GA_{ve} = GA_v \frac{EI_e}{EI_g} \qquad \text{(Equation 4)}$$

For cap beams that are monolithically integrated into the superstructure, the effective width of cap beam should be employed. It was necessary to account for enhancement of stiffness and capacity due to the contribution of the deck and soffit slab in box girders to the flexural stiffness. In the assessment model, a larger effective width was estimated by assuming a 45° spread of tributary force flow (Priestley, 1996).

MODELING OF SPREAD FOOTINGS

Bridge foundations are generally stiffer than columns or bents and may be assumed to be rigid. From the literature, the load-deformation behavior of foundations has been recognized to be nonlinear. In the National Earthquake Hazards Reduction Program (NEHRP) Guidelines (FEMA-273, 1997), an equivalent elasto-plastic representation of load-deformation behavior is recommended for most foundation systems. Because properties of the soil supporting foundations is highly variable and static foundation loads are difficult to determine, an upper and lower bound approach to defining stiffness and capacity is also recommended.

In this research, the foundations investigated are shallow bearing foundations, which are stiffer when compared with the soil upon which they rest. By running test models, very small displacements were detected for the movement of foundations, which means the foundation could be modeled using linearly elastic springs. However, an upper and lower bound in the stiffness approach is still employed to estimate the parameter variability, which is addressed in the parametric study presented in Chapter 5.

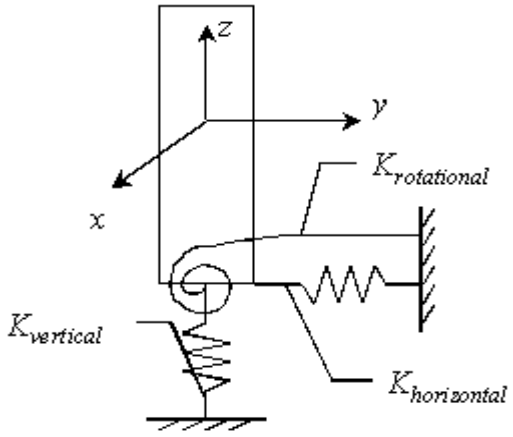

Figure 6. Uncoupled foundation spring model (FEMA-273, 1997)

An uncoupled spring model recommended by the National Earthquake Hazards Reduction Program (NEHRP) Guidelines (FEMA, 1997) is employed. Equivalent static spring constants are used, by which results are reasonably insensitive to repeated loading conditions. Equivalent spring constants can be calculated using conventional theoretical solutions for rigid plates resting on a semi-infinite elastic medium. Parameters related to spring stiffness include the soil modulus of elasticity, E, soil Poisson's ratio, ☒, dimensions of the foundation and the embedment depth. Elastic solutions for the spring constants are provided in the NEHRP Guidelines (FEMA-273, 1997). Rectangular foundation plates are calculated and transformed into an equivalent circular section as

shown in Figure 7. Based on the equivalent circular footing, the stiffness of translation and rotation is determined. Stiffness constants are adjusted for shape and depth by a shape factor, α , and an embedment factor, β , which are given in the Appendix.

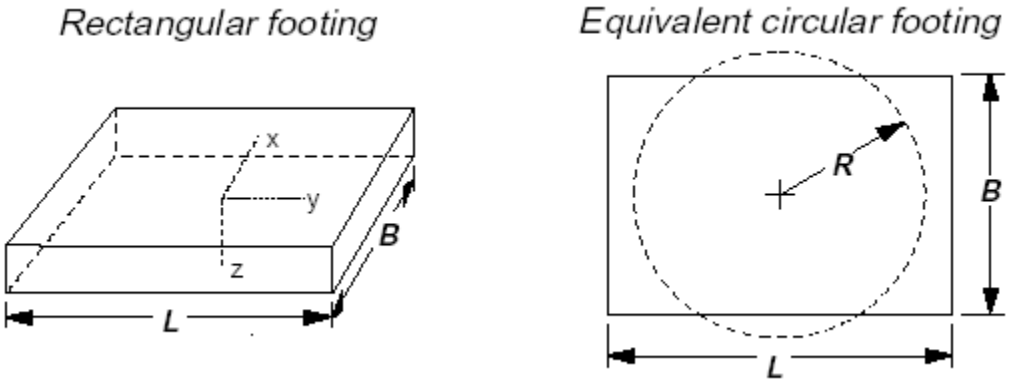

Figure 7 Radii of circular footings equivalent to rectangular footings (FEMA-273, 1997)

The equivalent radius, R, was estimated for translational and rotational degree of freedom using the following formulas in Table 1, in which *B* is the footing width and *L* is the footing length along *y* direction.

Table 1 Equivalent radii calculation equations

	Translational Direction	Rocking about x-axis	Rocking about y-axis	Torsion
Equivalent Radius *R*	$\left(\frac{BL}{\pi}\right)^{\frac{1}{2}}$	$\left(\frac{BL^3}{3\pi}\right)^{\frac{1}{4}}$	$\left(\frac{B^3L}{3\pi}\right)^{\frac{1}{4}}$	$\left[\frac{BL\left(B^2+L^2\right)}{6\pi}\right]^{\frac{1}{4}}$

The shear modulus, G, for a given soil is obtained from the modulus of elasticity and Poisson's ratio by the relationship given by Equation 5 (FEMA-273, 1997).

$$G = \frac{E}{2(1+\nu)} \qquad \text{(Equation 5)}$$

Poisson's ratio can be taken as 0.35 for unsaturated soils and 0.50 for saturated soils. As the geo-technical information for this study is not available, a value of 0.35 is conservatively used for all of the models in this research. Further parametric study is conducted on foundation spring stiffness constants to estimate their influence to the lateral displacements of bridge.

Stiffness coefficients for the equivalent circular footing are estimated using the equations in Table 2 (FEMA-273, 1997). It is used to calculate the spring constants for

rectangular footings, k, with the relationship that $k = \alpha\beta k_0$, in which α and β are adjusting factors as explained previously.

Table 2 Stiffness coefficient for footing from the equivalent circular footing:

Direction	Vertical translation	Horizontal translation	Torsional rotation	Rocking rotation
Spring stiffness k_0	$\frac{4GR}{1-\nu}$	$\frac{8GR}{2-\nu}$	$\frac{16GR^3}{3}$	$\frac{8GR}{3(1-\nu)}$

MODELING OF ABUTMENTS

The most commonly seen abutments in older bridges include monolithic or diaphragm and seated abutments. In these two types, the superstructures are built either monolithically or separated by joints and bear upon the back wall. The effect of abutments on the response of a bridge is related to its geometry and mass as well as surrounding soil properties.

Analytical response of bridges can be significantly affected by the modeling characteristics of the abutment stiffness and capacity, which can be very complicated. This is due to the large soil mass that interacts with the abutment and the abutment geometry, which exhibits higher stiffness values than other bridge bents. These reasons result in more seismic forces to be attracted to the abutment. Another difficulty in modeling abutments is that the soils and piles behavior present a high variability and may produce a highly nonlinear behavior in large seismic event. Hence, in most cases abutment stiffness characteristics are determined based on empirical relationship or experiment results.

Large-scale abutment tests were conducted in UC Davis (Kutter, et al., 2003). Results from these experiments can be used to more realistically establish force displacement relationship of the abutment. The characterization is in the direction that the abutment backwall is fully engaged in the push movement. Figure 8 is a proposed trilinear force-deformation relationship, in which the lateral-axis is the ratio of abutment longitudinal deformation to abutment height, and the vertical-axis is force applied on unit area (Priestley, 1996).

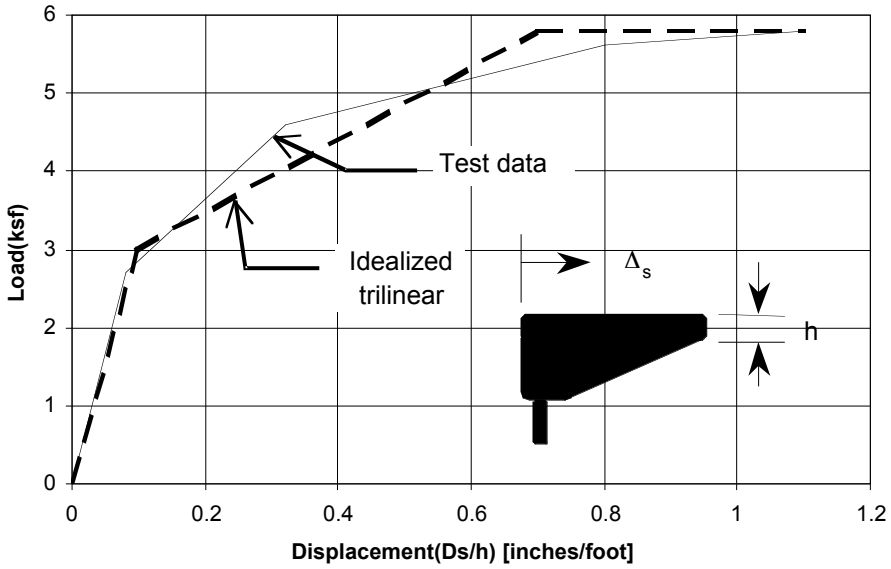

Figure 8 Proposed characteristics and experimental envelope for abutment backwall load deformation (adopted from Priestley, 1996)

Due to the variability of soil property and various types of abutment, the longitudinal stiffness obtained from the UC-Davis may not be precise. In Chapter five, the longitudinal stiffness is studied as a parameter to estimate its influence on the bridge response. The above force-displacement relationship provided a baseline for the study.

The nonlinear relationship of force and abutment displacement in the transverse direction is difficult to determine. Resistance is not only coming from the wingwall and the surrounding soil, but also relates to the adjacent bent stiffness. Often, a linear force-displacement relationship is proposed, but it cannot capture the inelastic response of the shear keys, wingwalls and piles. Insufficiency of information on local soil properties and construction details placed more difficulties on accurately estimating transverse abutment stiffness. The trilinear relationship obtained from UC-Davis was employed again and results were used as a baseline for further parametric studies on the transverse abutment stiffness.

PLASTIC HINGE

Moment Curvature Relationship Of A Section

It is well known that well-confined concrete structures can deform inelastically without significant strength loss through several cycles of response. Ductility describes such ability of structures, which is often defined as the ratio of deformation at a given response level to the deformation at yield response. Commonly used ductility ratios

include displacement ductility, curvature ductility and rotation ductility. In the software of XTRACT, developed by Imbsen & Associates Company (2002) with the capability of analyzing structural cross sections, curvature ductility can be calculated for a given section and are defined in Equation 6 (Paulay and Priestley, 1992).

$$\mu_{\phi} = \frac{\phi_u}{\phi_y} = \frac{\phi_p + \phi_y}{\phi_y} \qquad \text{(Equation 6)}$$

in which ϕ_y is yield curvature, ϕ_p is plastic curvature, and ϕ_u is summation of yield curvature and plastic curvature that presents the ultimate curvature capacity of a section.

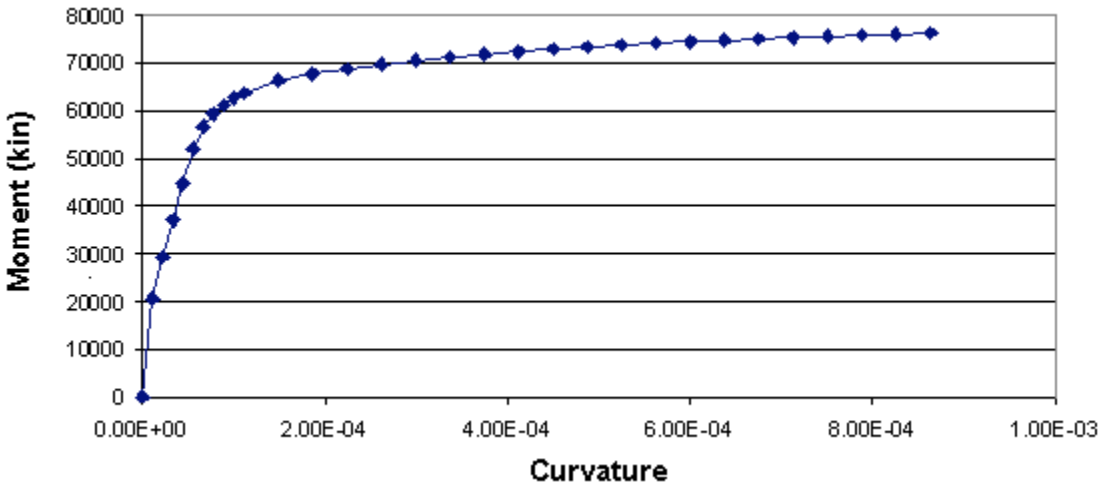

Figure 9 Moment–curvature curve of built-in columns sections of the Dry Wash

Figure 9 gives a moment-curvature diagram for the column section in the Dry Wash Bridge, calculated by the XTRACT. Curvature properties are section dependent and can be determined by numerical integration methods. Input data of a cross-section include nonlinear material properties of concrete and steel, and the detailed configuration of the section. For the Dry Wash Bridge, all the columns have the identical section dimension, however, the moment-rotation relationships may not be the same because of the different axial loads.

Concrete Compression Strength

By its definition, the nominal strength is 20 to 25% lower than the actual compressive strength, which should be considered in an analysis model. In addition, the compression strength of concrete is affected by two factors, which if not considered, would be too conservative when nominal strength is taken. The first is the strength concrete increases with age for old bridges. In California tests on cores of concrete taken from bridges constructed in 1950s and 1960s have shown a 50% to 170% increase in

strength (Priestley, 1996). To account for a safety reduction of nominal value and strength enhancement due to age, in this study a conservative average value of 1.5 times the nominal compressive strength is used. In addition to strength enhancement due to age, lateral confinement also increases compression strength and ultimate strain. The enhanced concrete compression strength by confinement, f'_{cc}, is related to the yield strength and effective volumetric ratio of confining steel, and the concrete strength f'_c. It can be estimated utilizing Figure 10 according to Priestley (1996).

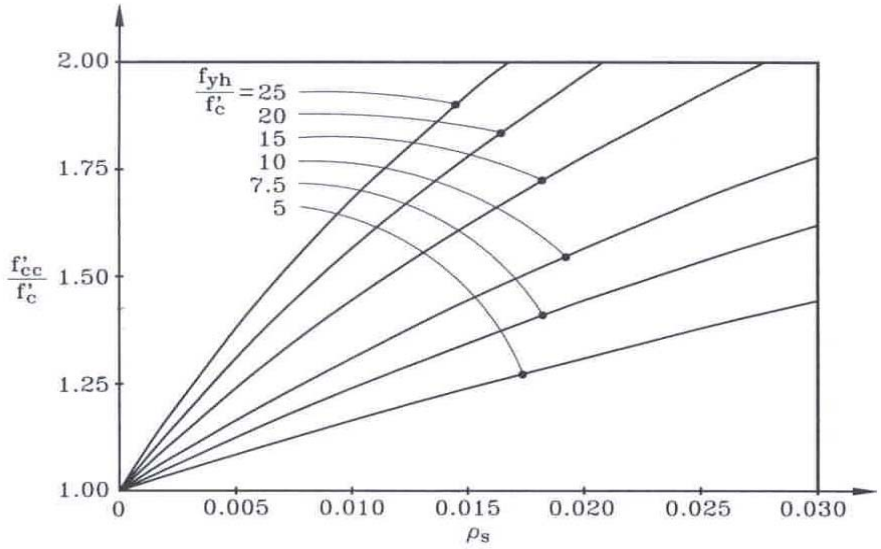

Figure 10 Enhancement of concrete compression strength by confinement (Priestley, 1996)

The effective volumetric ratio of confining steel, ρ_s, for circular columns can be calculated as $\rho_s = \frac{4A_{sp}}{D's}$, where A_{sp} is the bar area of spiral reinforcement, D' is core diameter of circular columns, and s is longitudinal spacing of the hoop or spiral.

Concrete Ultimate Compression Strain

In flexural strength calculations, a compression strain of 0.003 is used as the maximum compression strain. However, this does not reflect the ultimate condition of the extreme fiber compression, in which strain can be as high as 0.02. The use of ε_c=0.003 is too conservative, and if a nominal material strength is simultaneously used to calculate ultimate moment capacity, the conservatism will be substantial. Hence, ultimate compression strain of concrete should be estimated with consideration of the enhancement due to lateral reinforcement and confinement by adjacent members such as footings or cap beams, given as Equation 4-6 (Priestley, 1996).

$$\varepsilon_{cu} = 0.004 + \frac{1.4\rho_s f_{yh}\varepsilon_{su}}{f'_{cc}} \qquad \text{(Equation 7)}$$

ε_{su} is the steel stain at maximum tensile stress, f'_{cc} is confined concrete strength and f_{yh} is yield strength of transverse reinforcement.

The above equation is for typical circular reinforced concrete columns. For steel jacketed circular reinforced concrete columns, the steel jacket is the main confinement. In that case, the maximum compression strain of concrete is closely related to the properties of the jacketing steel. The thickness of the steel jacket, tj, can be obtained by Equation 4-7 (Priestley, 1996).

$$t_j = \frac{0.18(\varepsilon_{cm} - 0.004)Df'_{cc}}{f_{yj}\varepsilon_{sm}} \qquad \text{(Equation 8)}$$

where ε_{cm} is the maximum compression strain, and can be assumed as 0.015 for first trial to design a steel jacket. After t_j is determined by a trial-and-error process, the actual maximum strain can be estimated by Equation 4-8 (Priestley, 1996).

$$\varepsilon_{cu} = 0.004 + \frac{5.6t_j f_{yj}\varepsilon_{sm}}{Df'_{cc}} \qquad \text{(Equation 9)}$$

in which f_{yj} is the yield stress of jacketing steel with strain at maximum stress of ε_{sm}.

In XTRACT (2002) properties of cover concrete (unconfined concrete) and core concrete (confined concrete) are separately inputted. To insure section failure occurs when ultimate strain in the core concrete is reached, an unrealistically large strain capacity such as 1, is given to the cover concrete to avoid section failure in the cover concrete. When modeling a steel jacketed column, similar method was taken to avoid the program stopped due to excessive cover concrete deformation. In a jacketed column, longitudinal reinforcement failure could become the reason of the section failure.

Plastic Hinge And Strain Penetration

The plastic hinge is a region of plasticity over which inelastic rotation will occur without significant strength loss. Reinforcing detailing requirement must be met over this region to ensure inelastic rotation capacity. At maximum flexural response of a column, curvature over the plastic hinge region is the summation of yield curvature and plastic curvature, which is substantially larger than the yield curvature. For a simple structural

element, such as a cantilever beam, the distribution of curvature and plasticity can be illustrated in Figure 11.

Deflection at the free end of the beam can be estimated as $\Delta_m = \int \phi(x) x dx$, where $\phi(x)$ is the curvature distribution at maximum response. Maximum curvature and yield curvature are ϕ_m and ϕ_y respectively. For simplicity, plastic curvature ϕ_p is assumed equal to $(\phi_m - \phi_y)$ and remains constant over an equivalent length L_p, so that the plastic displacement at the top end of the cantilever beam can be predicted by the simplified approach and remains the same as that derived from the actual curvature distribution. The equivalent plastic hinge length L_p, however, is not the experimentally measured length of plasticity. It is a theoretical value based on integration of the curvature distribution for typical members to predict the element displacement. A good estimate of the equivalent plastic hinge length obtained from analyses and test results is given by Equation 4-9 (Paulay and Priestley, 1992):

$$L_p = 0.08L + 0.15 f_{ye} d_{bl} \geq 0.3 f_{ye} d_{bl} \quad (f_{ye} \text{ in kis}) \qquad \text{(Equation 10)}$$

In the above equation, L is the distance from the critical section of the plastic hinge to the point of contraflexure, and d_{bl} is the diameter of the longitudinal reinforcing bars. The second term in the above equation accounts for the phenomenon of tensile strain penetration. The strain penetration length L_{pj} can be estimated by Equation 4-10 (Priestley, 1996).

$$L_{pj} = 0.15 f_{ye} d_{bl} \qquad (f_{ye} \text{ in ksi}) \qquad \text{(Equation 11)}$$

The extent of strain penetration is related to reinforcing bar size, because the development length of the longitudinal rebar is proportional to bar size. Tensile strain penetration allows for additional rotation and deflection beyond the theoretical base into the supporting element as a result of the elongation of longitudinal bars. This is also one of the reasons why displacements from integration of theoretical curvature distribution are not consistent with the experimental measurements. The theoretical curvature distribution ends abruptly at the end of the cantilever, while in actuality longitudinal steel tensile strain extends into the footing. A relation of extent of plasticity, equivalent plastic hinge length, and strain penetration is illustrated in Figure 11.

It is obvious that yield strain penetration extending into adjacent members provides additional flexibility, and can be conveniently expressed by an increase of effective column height H_e from clear column height H_c. In double bending of bridge columns, plastic hinges are expected to form at one or both ends of the column member, so yield penetration of column longitudinal reinforcement will extend into adjacent footing or cap beam and provide additional flexibility to these regions.

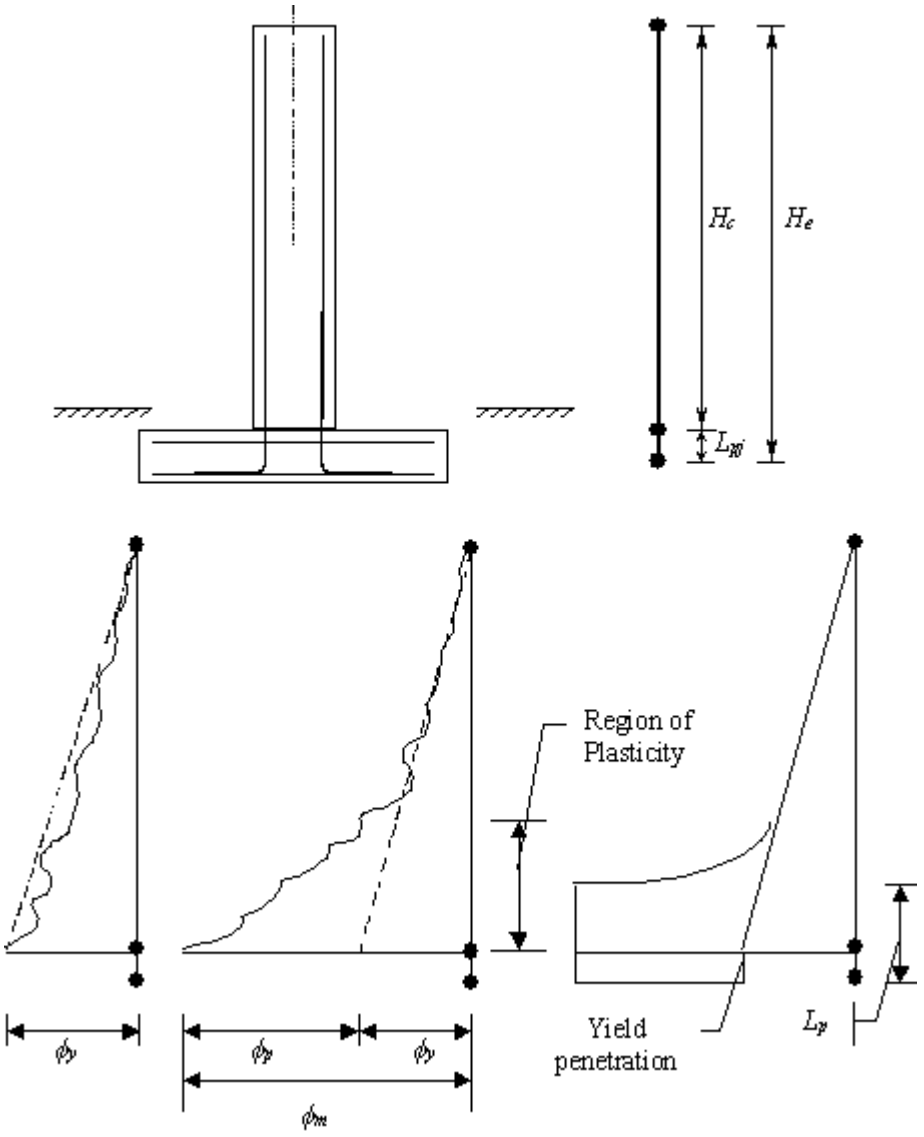

Figure 11 Relationship of curvature and plasticity of a cantilever beam (Paulay and Priestley, 1992)

The yield penetration length is to be added to the clear column height H_c to form the effective column height H_e. Figure 12 shows the H_e, footing springs modeling the effects of soil deformations and location of plastic hinges, which are in red dots.

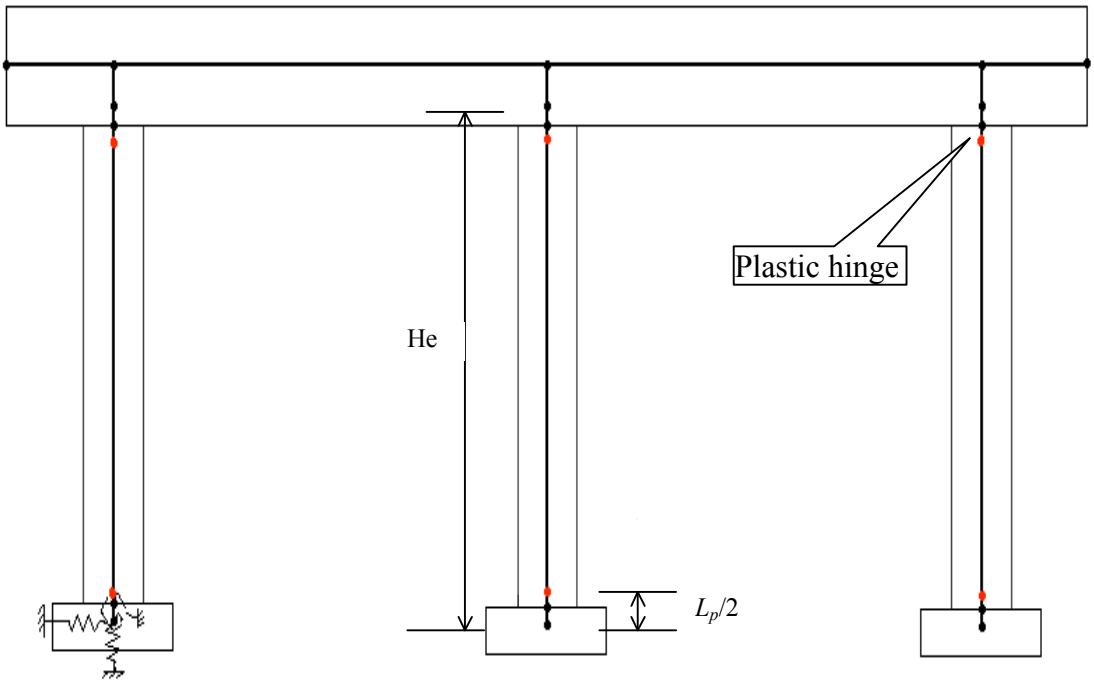

Figure 12 Model of Bent 2 of Dry Wash Bridge created by SAP

For steel jacketed columns, the gap between the steel plate and the adjacent member should be added to the plastic hinge length. In actuality, the plasticity concentrates at the gap, with the strain penetration extending on either side of the gap. Hence, the equivalent plastic hinge length for jacketed columns would be estimated with Equation 4-11, in which g is the gap length.

$$L_p = g + 0.3 f_y d_{bl} \qquad (f_y \text{ in ksi}) \qquad \text{(Equation 12)}$$

The location of the plastic hinge is still half the plastic hinge length away from the end of the effective column height. Since the tensile strain penetrate above and below the gap is the same length, the middle point of the plastic hinge becomes the center of the gap.

Plastic Hinge Property

The Manual of SAP (2000) recommends a distributed plastic hinge model assuming 0.1 of element length as the plastic hinge length, but information on how to define distributed plastic hinge properties is not provided. In this research, a concentrated plastic hinge model is used with the assumption that plastic rotation will occur and concentrate at mid-height of a plastic hinge. Point hinges are located at half of

the plastic hinge length away from the end of the effective column element as shown in Figure 12. Input hinge properties consist of the section yield surface, plastic rotation capacity, and acceptance criteria.

A plastic rotation, θ_p, can be calculated by the plastic curvature given the equivalent plastic hinge length L_p as shown in Equation 4-12.

$$\theta_p = \phi_p L_p = L_p(\phi_u - \phi_y) \qquad \text{(Equation 13)}$$

The plastic rotation is an important indicator of the capacity of a section to sustain inelastic deformation and is used in SAP to define column plastic hinge properties. FEMA 356 (1997) provides a generalized force-deformation relation model shown in Figure 13 for the nonlinear static analysis procedure, which is the defaulted model in SAP for the Axial-Moment hinge.

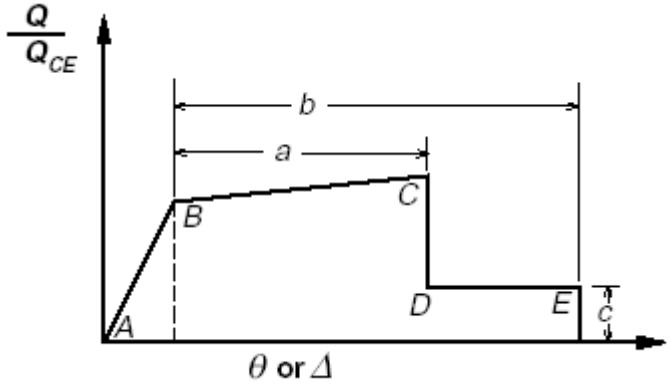

Figure 13 Generalized force-deformation relations for concrete elements (FEMA-356, 2000)

Three parameters, *a*, *b* and *c* are defined numerically in FEMA-365 (2000), and are permitted to be determined directly by analytical procedures. The moment and rotation are normalized by yield moment and yield rotation respectively, i.e., $\frac{M}{M_y}$ and $\frac{\theta}{\theta_y}$. By default SAP will calculate the yield forces and the yield rotation based on reinforcement and section provided.

In Table 6-8 of FEMA 356 (2000), modeling parameters and numerical acceptance criteria are given for reinforced concrete columns in various categories. Columns investigated are all primary structural elements. A conforming transverse reinforcement is defined by hoops spaced in the flexural plastic hinge region less than or equal to $\frac{d}{3}$, and the strength provided by the hoops (*Vs*) being greater than three-fourths of the design

shear. Thus, the category of the column is decided in Table 6-8 of FEMA 356 (2000), and values and relationship of the performance levels can be utilized.

In SAP, an absolute rotation value can overwrite the default value in defining a hinge property. The plastic rotation capacity angle, *a*, calculated with Equation 4-12 for a given column is at point C. The ultimate rotation angle, which is inputted as *b* in SAP, is taken as 1.5 times the plastic angle. It is indicated at point E, which defines a local failure at a plastic hinge. A larger value could be used to allow the structure to form a global failure due to instability.

The three discrete structural performance levels are Immediate Occupancy (IO), Life Safety (LS) and Collapse Prevention (CP) shown in Figure 14.

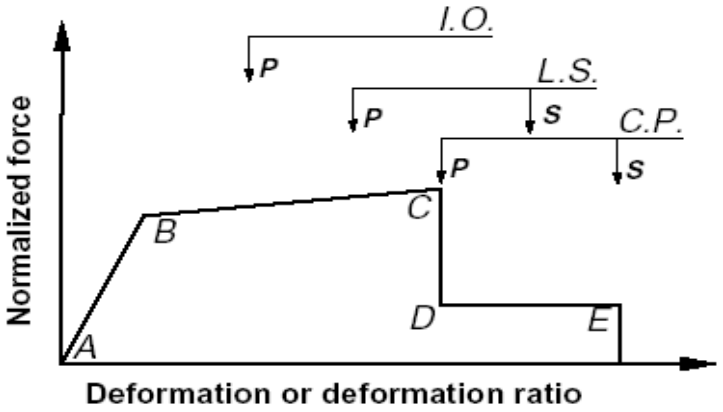

Figure 14 Performance level on Generalized force-deformation relations for concrete elements (FEMA-356, 2000)

The ultimate plastic hinge angle calculated by the XTRACT was taken as the Collapse Prevention level. Its value was indicated as "*a*" in Figure 13. The permissible deformation for the Life Safety performance level is taken as three quarters of the plastic rotation capacity "*a*".

The increase of moment strength at point C is taken as the over strength factor computed by XTRACT, ignoring the strength softening effect. The actual moment strength at point C is the product of the factor and the yielding moment. FEMA 356 (2000) defines a 0.2 residual strength ratio before plastic hinge eventually fails. Figure 15 presents moment-rotation curves for one of the columns in Dry Wash Bridge.

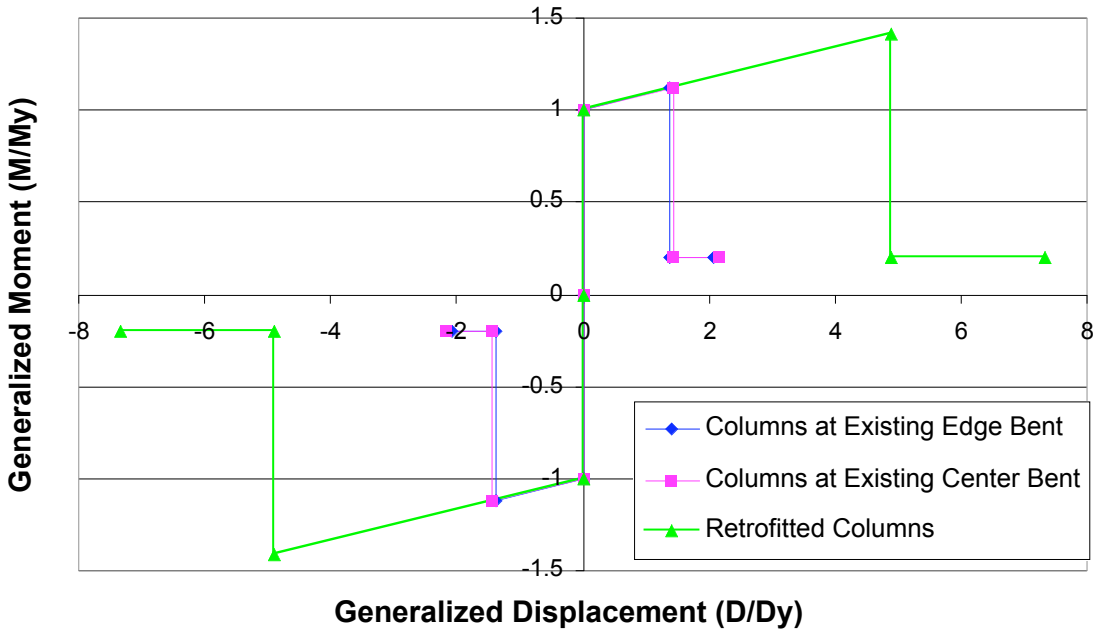

Figure 15 Moment-Rotation relationship of the columns of Dry Wash Bridge

A defaulted concrete interaction surface obtained from ACI 319-95 (ACI, 1995), with _=1 is used for the frame hinge under combined bending and axial load. A generated interaction surface is shown in Figure 16.

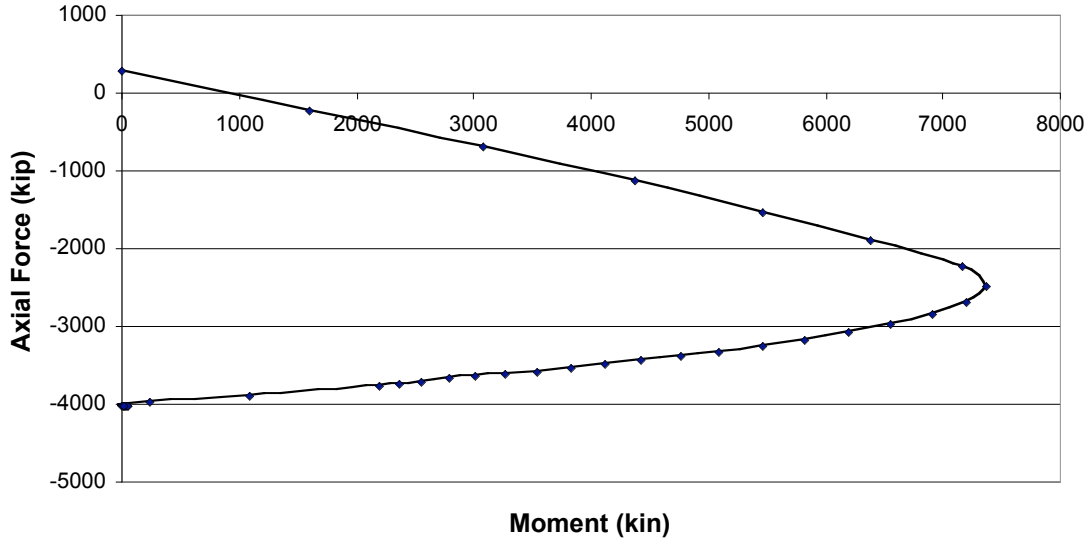

Figure 16 Axial load-Moment interaction curve for columns of Dry Wash Bridge (Compression force is negative in the above figure)

DESCRIPTION OF THE DRY WASH BRIDGE

The Dry Wash Bridge is located in the town of East Wenatchee, Washington. It is a four-span reinforced concrete bridge with multi-cell box girders. It has no skew along longitudinal direction or along the bent axis. The total length of the bridge is 288 feet. The bridge was constructed in 1974 under revised seismic design methods.

Figure 17 Dry Wash Bridge in the town of East Wenatchee, WA.

Figure 17 shows a photograph of the bridge. A plan-view drawing of the bridge and the site topography are given in the Appendix. The reinforced concrete deck is continuous, spreading from the west to the east, with a width at the west end of 89 feet and 108 feet at the east end. The bents and the cap beam were cast monolithically with box girder slabs and columns. Thus the lateral loading of superstructure can be transferred to the bents and the abutments. The abutment is a cast-in-place diaphragm abutment.

Three bents support two center spans with lengths of 93 feet and 130 feet. The adjoining end spans are 30 and 35 feet long, supported by the bents at one end and abutments at the other. Each bent consists of three supporting circular columns that have outside diameters of 60 inches. Twenty-one No. 11 Grade 60 bars evenly spaced around the cross section perimeter provided the longitudinal reinforcement. Column transverse reinforcement consists of No. 4 hoops spaced at 6 inches, which provides good lateral strength and confinement. The spread footings are very similar but not in the exactly same size. For simplicity, they were regarded as 15 feet by 16 feet in plan and 3 feet deep. Details of bridge bents and footings are in the Appendix.

The majority of the concrete used in the bridge was WSDOT class AX mix, which has a specified compressive strength at 28 days, f'_c, of 4000 psi. The footings were constructed of WSDOT class B mix with a specified compressive strength of 3000 psi. The

steel rebars used are ASTM A-615, Grade 60, with a yield strength of f_y=60ksi. The maximum design soil pressure per square foot is five tons.

The calculations for different modeling components of the Dry Wash Bridge are in the Appendix.

RESULTS AND ANALYSIS

MODAL ANALYSES

Before the pushover analysis, a modal analysis was conducted to determine fundamental modal shapes and modal participating mass ratios so that a loading configuration could be established. The results of modal analysis of Dry Wash Bridge are listed below.

The fundamental mode in the longitudinal direction had a period of 0.43 second and excited 95.96% of the system mass in the longitudinal direction and 0% in the transverse direction. All the remaining modes individually excited less than 1% of the system mass in the longitudinal direction.

The fundamental mode in the transverse direction had a period of 0.63 second and excited 97.08% of the system mass in the transverse direction and 0% in the longitudinal direction. All the remaining modes excited less than 1% of the system mass in the transverse direction.

Modal analyses of different models corresponding to varying parameters are listed in In **Error! Not a valid bookmark self-reference.**, the first row is the baseline response of the Dry Wash Bridge. It can be seen that Mode 3 excited 97.78% system masses to move in the longitudinal direction. And Mode 1 excited 97.49% system masses to move in the transverse direction. By varying foundation stiffness and abutment link element stiffness, a class of structure was generated based on the baseline bridge. Their modal characterization shared the similarity that over 95% system masses were excited to participate in the vibration of one direction. This indicates that the nodes along the superstructure tended to move in constraints in the fundamental modes.

Table 3. In both the longitudinal and the transverse directions, the fundamental periods were short. Movement associated with large system masses tended to concentrate in one mode in each direction. Therefore, higher mode effects were assumed to be negligible. Pushover loadings were applied based on the modes that associated with the largest mass participation ratio.

In **Error! Not a valid bookmark self-reference.**, the first row is the baseline response of the Dry Wash Bridge. It can be seen that Mode 3 excited 97.78% system masses to move in the longitudinal direction. And Mode 1 excited 97.49% system masses to move in the transverse direction. By varying foundation stiffness and abutment link element stiffness, a class of structure was generated based on the baseline bridge. Their modal characterization shared the similarity that over 95% system masses were excited to participate in the vibration of one direction. This indicates that the nodes along the superstructure tended to move in constraints in the fundamental modes.

Table 3 Periods and mass participation ratios of models with varying parameters

Model		Mode number	Period with the largest mass participation (s)	Mass excited in longitudinal direction	Mass excited in transverse direction
Baseline model		3	0.43	97.78%	0
		1	0.63	0	97.49%
Abutment rotation restrained		3	0.35	96.37%	0%
		1	0.51	0	97.56%
Fixed-end foundation model		3	0.40	97.21%	0
		1	0.53	0	96.23%
Soft foundation modal		1	0.76	96.93%	0
		3	0.46	0	97.81%
Pinned-end foundation model		3	0.43	97.65%	0
		1	0.59	0	97.92%
Varying abutment longitudinal spring stiffness	Link 1	1	0.83	97.90%	0
		2	0.74	0	97.57%
	Link 2	1	0.82	97.90%	0
		2	0.74	0	97.57%
	Link 3	3	0.82	97.90%	0
		1	0.74	0	97.57%
Varying abutment transverse spring stiffness	Link 1	1	0.83	96.39%	0
		2	0.74	0	97.57%
	Link 2	1	0.83	97.90%	0
		2	0.74	0	97.57%
	Link 3	3	0.82	97.90%	0
		1	0.74	0	97.57%

VALIDATION OF MODELING ASSUMPTIONS

It was assumed that the influence of the rotational restraints of the abutment could be neglected. To validate the assumption that the abutments can be modeled as free of rotation restraints, two cases were compared. In the first case the rotation of abutments was fully restrained, and in the second case the abutments had no rotational stiffness. It can be seen from the results shown in Figure 18 and Figure 19 that the rotational spring stiffness had little effect on the response of the bridge when comparing the displacement at the monitored point resulting from the two models.

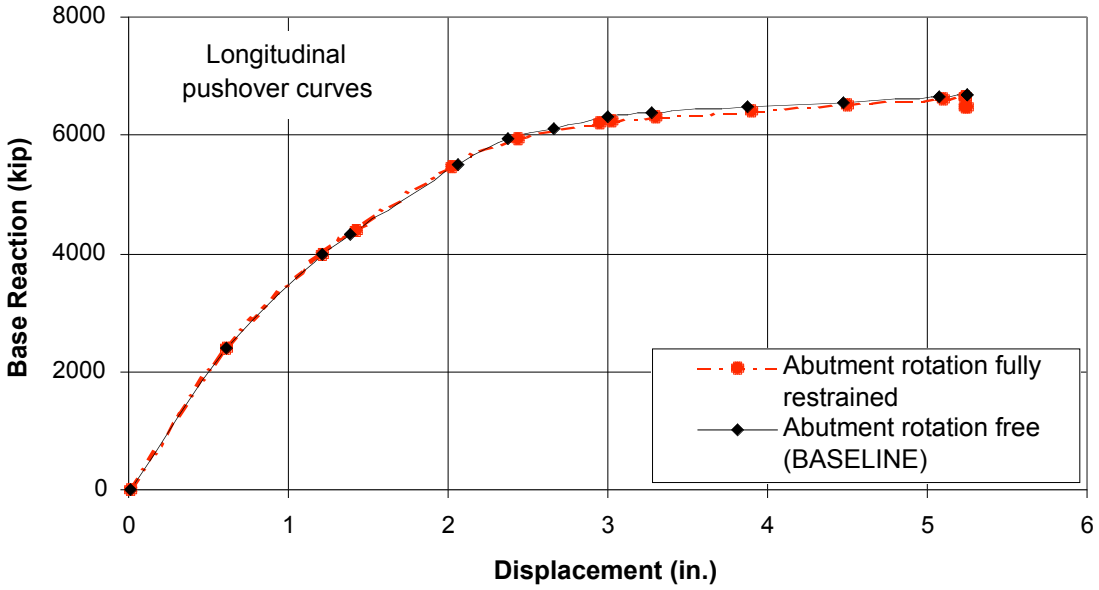

Figure 18 Longitudinal pushover curves of abutment rotation restraints test

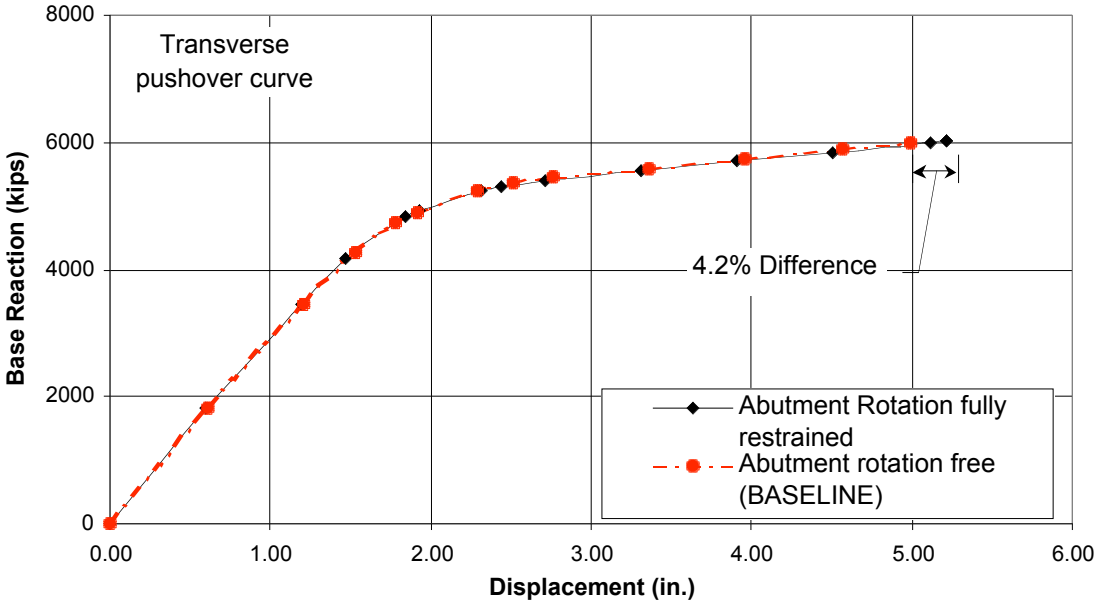

Figure 19 Transverse pushover curves of abutment rotation restraints test

In the longitudinal direction, the two pushover curves were identical. But transverse-wise, the structure tended to have a slightly larger displacement if the abutments were rotationally restrained. If the abutment could rotate freely, the transverse displacement was reduced 4.2%. This can be explained by Figure 20, in which the dashed

lines are the exaggerated deflection shapes of the superstructure under transverse modal loading.

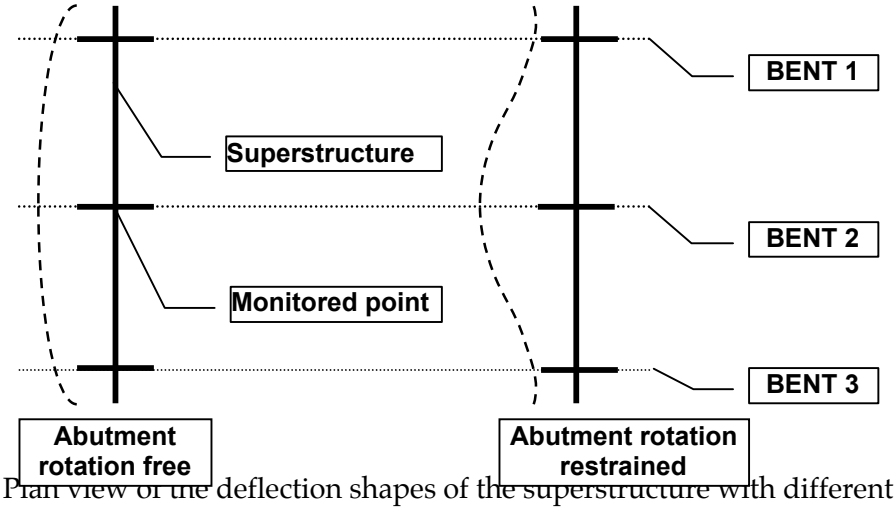

Figure 20 Plan view of the deflection shapes of the superstructure with different abutment restraints

In both cases in spite of the influence of the abutment rotation, the largest displacement along the superstructure occurred at the top of the Bent 2. By observing the collapse modes of the structure, it has been found that the bridge failed in the transverse direction due to hinge degradation at Bent 3. So the displacement of the top of the columns at Bent 3 controlled the failure of the structure. In the rotation-restrained model, the displacement at the top of Bent 1 and Bent 3 were reduced due to the restraints from the abutments in Figure 20 (right). In consequence, the rotation-restrained abutments allowed the Bent 2 to displace further transversely by postponing the Bent 3 to reach its rotation capacity.

Compared to the transverse displacement of the whole superstructure, the variation of the displacement at different bents shapes was very small. Therefore the rotational effects at the abutments can be ignored. This conclusion was supported by the fact that the same failure mechanism and the same sequence of the hinge yielding occurred in these two cases. Thus, the assumption is verified and in the following study no rotational springs were allotted to abutments.

RESULTS ANALYSIS OF DRY WASH PUSHOVER

Longitudinal Pushover Results Of Dry Wash And Explanations

Figure 21 shows the longitudinal pushover curve of the baseline model of Dry Wash Bridge overlaid by the single demand spectrum with variable damping. The demand spectrum was produced with the assumption that the bridge was in the Seismic

Design Category B as defined in the IBC code (2000). The last point on the pushover curve is regarded as the ultimate capacity point, which indicates a displacement of 5.24 inches, and a base force is 6678 kips. The single demand spectrum intersected with the pushover curve at the performance point (2.171 in., 5656kip). That means that a design level earthquake (B category) is expected to impose a displacement of 2.171 inches in this structure, which is 41.4% of its longitudinal displacement capacity.

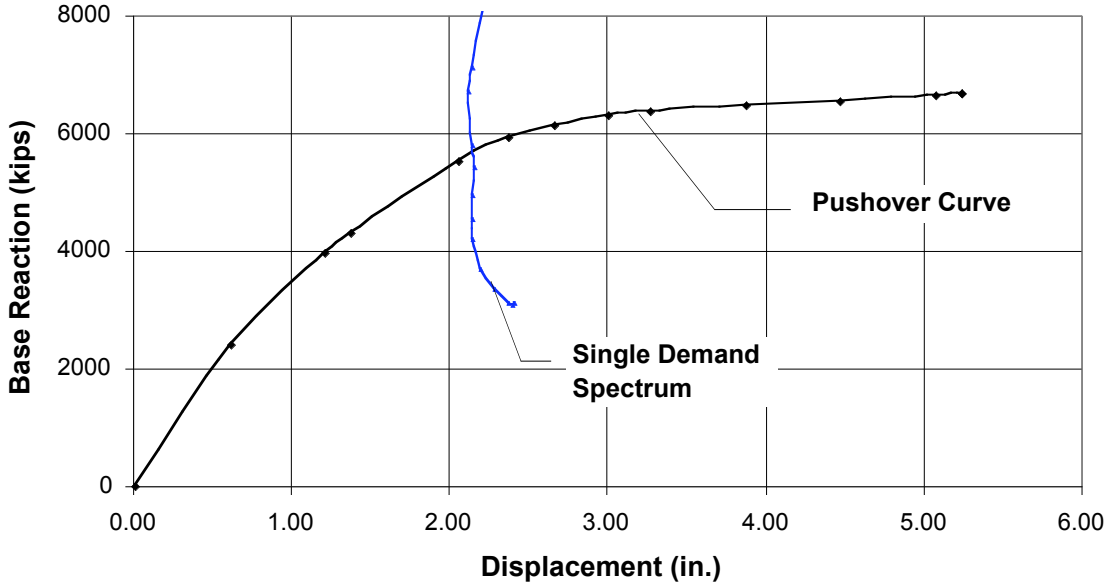

Figure 21 Longitudinal pushover curve of Dry Wash Bridge

The Dry Wash consists of nine columns, three columns at each bent. Eighteen plastic hinges were pre-assigned in the model. The formation of plastic hinges was in sequence shown in Figure 22 on a step-to-step basis. Some of the plastic hinges yielded simultaneously at a particular pushover step. The pushover curves do not present a very obvious yielding plateau because the hinges on multi-columns provided a continuous redundancy for the structure to avoid immediate strength losses.

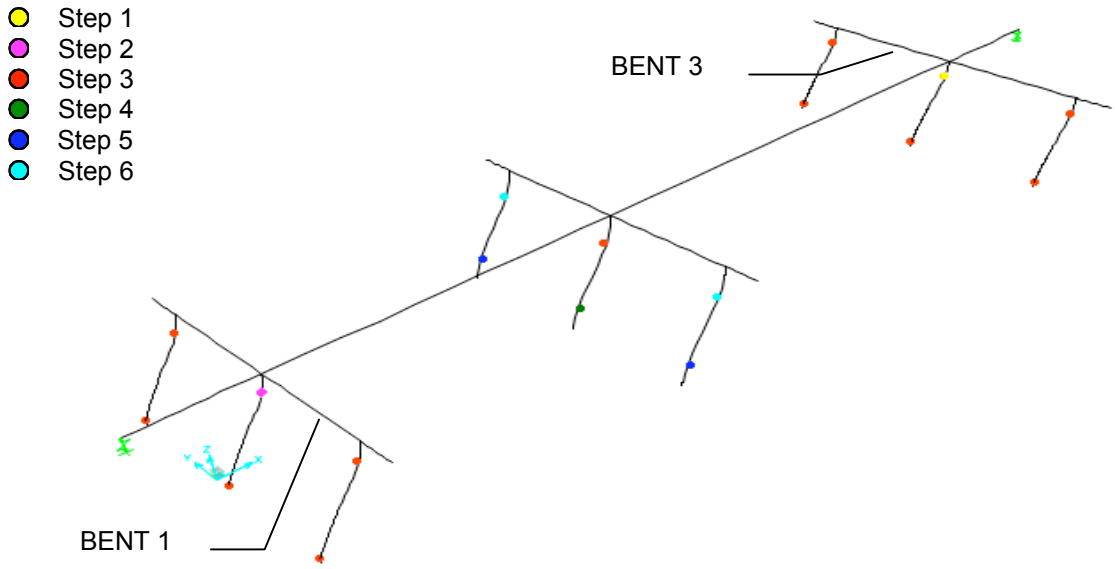

Figure 22 Dry Wash longitudinal pushover deflection and plastic hinges yielding sequence

The hinge at the top of the middle column at Bent 3 was the first yielded hinge. At step 6, all of the plastic hinges yielded, and the structure continued to push further until the last step, when hinges at the top of the middle columns at Bent 3 and Bent 1 failed as their rotation capacity were exceeded and 11 hinges were over their Life Safety level. As a result, the structure failed due to global instability. Table 4 shows the hinge statuses at yielding and ultimate step, in which A, B, C, D, E are points defining the moment-rotation relationship, and the Immediate Occupancy (IO), Life Safety (LS) and Collapse Prevention (CP) are performance levels as shown in Figure 14. Note that in defining the performance level in this study, the CP point was defined as the same point C. Point D represents the same rotation capacity with point C but with 80% strength degradation. So CP, C and D are at the same point on the moment-rotation relationship in this study.

Table 4 Hinge statuses Dry Wash Bridge at different steps in longitudinal pushover procedure

Steps	Displacement (in.)	Base Force (kips)	A-B	B-IO	IO-LS	LS-CP	CP-C-D	D-E	>E	TOTAL
Initial step	0.02	0.000	18	0	0	0	0	0	0	18
Yield step	1.38	4312.83	17	1	0	0	0	0	0	18
Ultimate step	5.24	6678.31	0	0	13	4	1	0	0	18

At the initial step the bridge displaced under its self-weight. The displacement of 0.02 inches shown in the initial step is the component displacement along the longitudinal direction of the bridge. Behavior of hinges under self-weight was still in linear range.

The yield point of the structure was defined as the point when the first yield occurred at one of plastic hinges, which is indicated in the table as the status of "B-IO".

A Capacity Spectrum of longitudinal pushover is shown in Figure 23. On the spectrum area, capacity spectrum and demand spectrum were plotted in the spectral acceleration versus spectral displacement coordinates. The blue line is the single demand spectra with variable damping, and the red lines are demand spectra with different damping ratios.

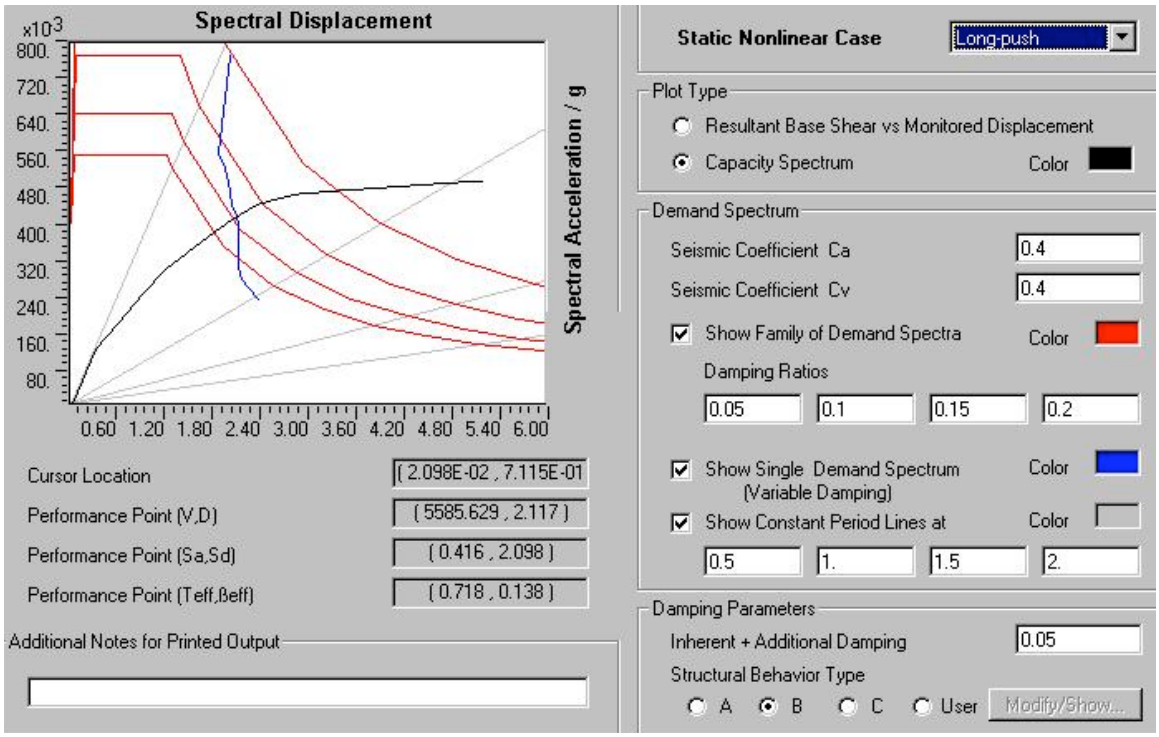

Figure 23 Longitudinal Capacity spectrum of Dry Wash.

Transverse Pushover Results Of Dry Wash And Explanations

In the transverse direction, the structure presented less displacement capacity compared to the longitudinal direction. It was assumed that the same seismic design category, B category, generated the single demand spectrum. The ultimate displacement was 5.00 inches, and the performance point was at (2.260in, 5226kip). So a design level earthquake can cause a displacement of 2.260 inches at the monitored point, which consumes 45.2% transverse displacement capacity of the bridge.

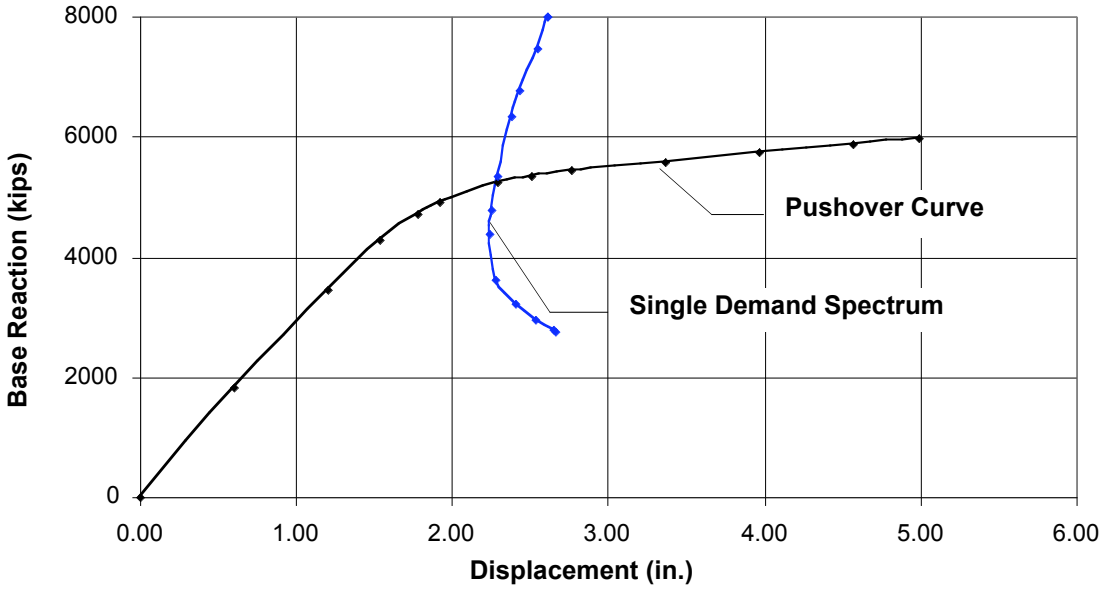

Figure 24 Pushover curve for Dry Wash Bridge on transverse direction

The hinges yielded in six steps shown in Figure 25. It has been observed that hinges at the edge bent yielded before those at the center bent. Hinges at the top of columns at Bent 3 yielded firstly.

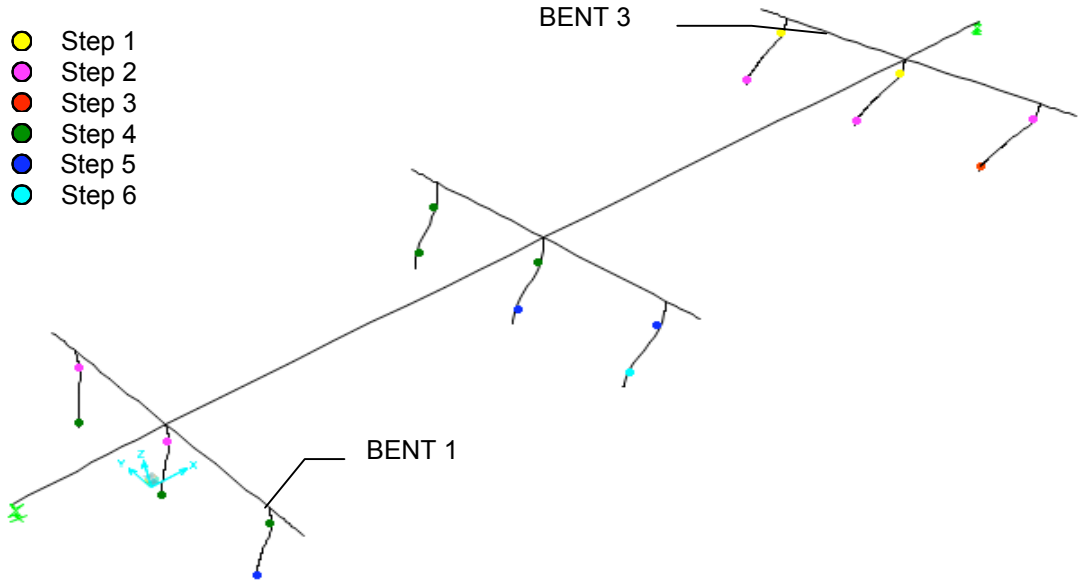

Figure 25 Dry Wash transverse deflection shape and plastic hinges yielding sequence

After the bridge displaced to its maximum capacity on the transverse direction, global instability was formed and the structure failed. The hinges statuses at yield and ultimate step are shown in Table 5.

Table 5 Hinge statuses of Dry Wash Bridge at different steps in transverse pushover procedure

Steps	Displacement (in.)	Base Force (kips)	A-B	B-IO	IO-LS	LS-CP	CP-C-D	D-E	>E	TOTAL
Initial step	0.005	0	18	0	0	0	0	0	0	18
Yield step	1.53	4373.93	16	2	0	0	0	0	0	0
Ultimate step	5.00	5991.12	0	0	10	7	1	0	0	18

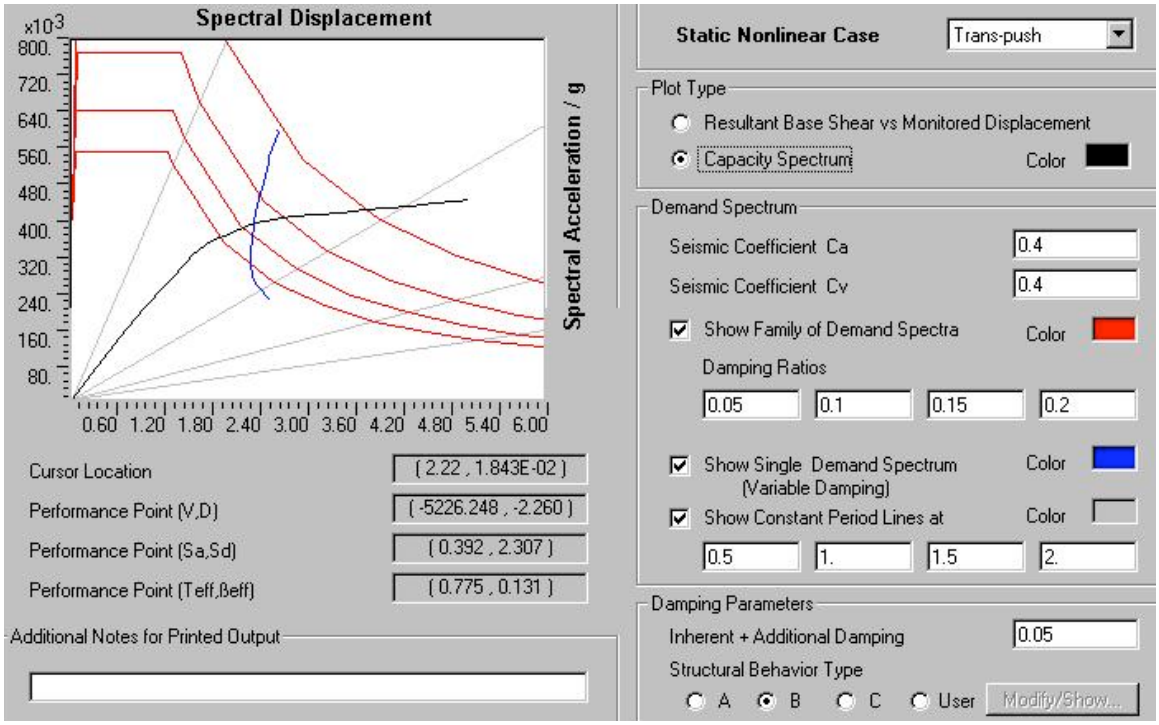

Figure 26 Transverse capacity spectrum of Dry Wash

Structural Ductility

Figure 27 compares the pushover curves and the relative locations of the performance points on the curves. It can be seen that the bridge was slightly less stiff in the transverse direction than the longitudinal direction. This is due to Dry Wash Bridge being better engaged with the backwall at the abutment than with the wingwall where the contact area with the soil was small.

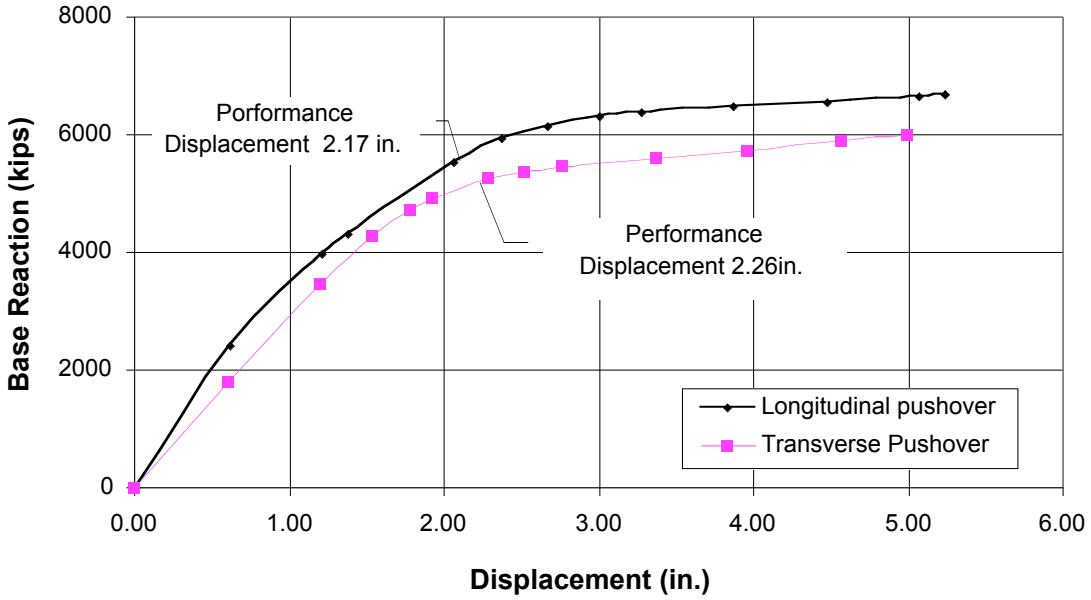

Figure 27 Comparison of the pushover curves of Dry Wash

In the longitudinal direction, the performance displacement is 41.4% of its ultimate capacity, while in the transverse direction the performance displacement is 45.2% of the ultimate capacity. This means that longitudinally the bridge has more displacement capacity reserved than that of transverse direction. Values of ductility are shown in Table 6. The bridge presented a better displacement ductility in the longitudinal direction than the transverse direction. Hence, retrofitting applications to enhance the transverse ductility have higher priority than applications aimed at longitudinal ductility enhancement.

Table 6 Structure ductility of Dry Wash Bridge

Dry Wash Bridge (baseline)	Yield displacement (in.)	Ultimate displacement (in.)	Displacement ductility	Performance displacement (in.)	Performance ductility
Longitudinal direction	1.38	5.24	3.80	2.17	2.41
Transverse direction	1.53	5.00	3.27	2.26	2.21

FOUNDATION STIFFNESS PARAMETRIC STUDY

As discussed in section 2.1.3, foundation rocking is one of the biggest problems for existing old bridges. However, if the bridge superstructure is continuous and the abutments are strong, the rocking can be allowed and be regarded as a form of seismic isolation by utilizing damping devices to limit the displacement. When the footing can provide sufficient strength capacity, locking the connection of the footing and the soil may not be necessary and desirable. However, due to the deficiency of the design philosophy that most old foundations were designed for gravity loading, some retrofitting actions have to be taken to increase the footing flexural strength and to limit excessive displacement that may induce to the superstructure. These retrofitting applications, represented in the bridge model, are the changes of foundation spring stiffness coefficients. Therefore, parametric study is performed on the spring constants of footings to test the global response of the full structure under the influence of the foundation retrofitting actions.

Three cases compose of this study. One is an extreme case by assuming that foundations are fully restrained in the six-degree of freedom, which is so called "fixed end". The second is so called "soft foundation". It is to calculate the spring stiffness coefficients with the previous equivalent circular footing method assuming that the columns had no bearing footings but were supported directly upon the soil. The third is to assume that the footings were pinned ended. Stiffness constants of the linear foundation springs for the three cases are listed in Table 7.

Table 7 Linear stiffness coefficients of soft foundation and rigid foundation

	k_x (k/in)	k_y (k/in)	k_z (k/in)	k_{rx} (k/rad)	k_{ry} (k/rad)	× (k/rad)
Pin-ended foundation	∞	∞	∞	0	0	0
Soft foundation	1328	1148	1072	3837895	2850361	3895315
Fix-ended foundation	∞	∞	∞	∞	∞	∞

The pushover curves of the three cases are compared with the baseline curve in Figure 28 (longitudinal direction) and Figure 29 (transverse direction).

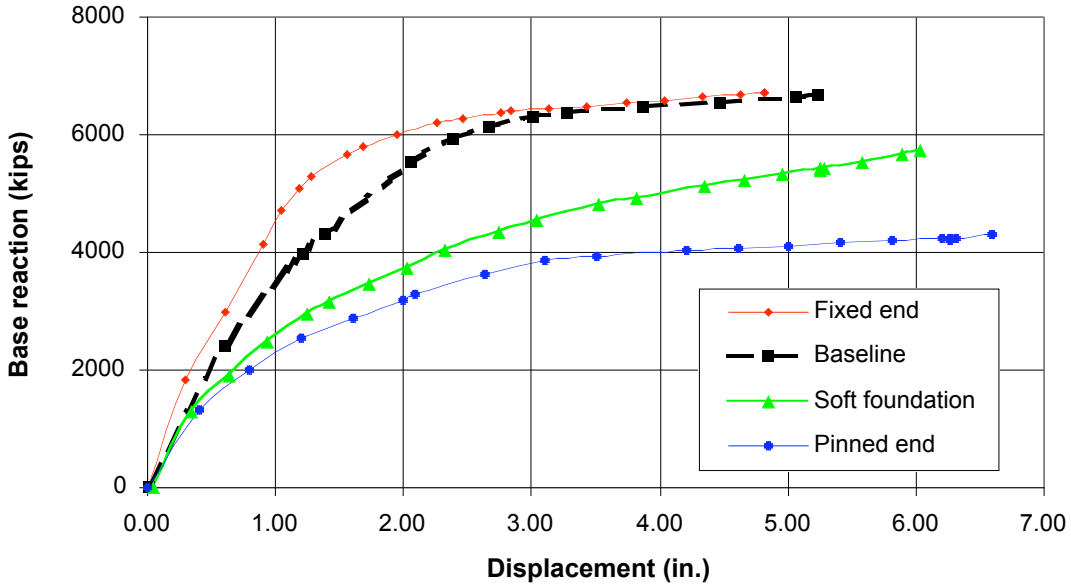

Figure 28 Longitudinal pushover curves of varying foundation stiffness models

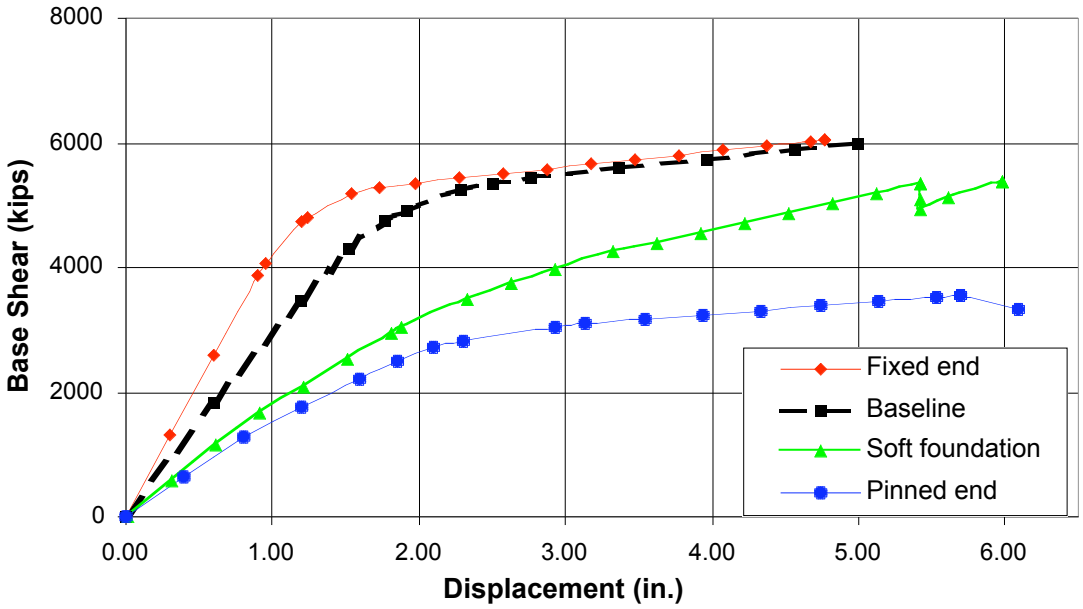

Figure 29 Transverse pushover curves of varying foundation stiffness models

It is obvious that rigid foundation yielded a stiffer response of the full structure and produced a more obvious yielding plateau. In the longitudinal direction, by increasing the foundation stiffness from the baseline to infinite rigid, the full structure represented an increase of 12% in its stiffness, and the ultimate displacement was reduced 8.2% from 5.24 inches to 4.81 inches. If the foundations were pinned ended, the performance force demand was reduced by 40% from the baseline and the displacement

increased by 26%. Yielding of bridges built upon softer foundations was postponed, because the soft foundations allowed the footing to rotate in addition to the rotation occurred within column. This means that the rotation demand was shared by and shifted to the footings. Figure 30 shows the deflection of the two cases, in which the left figure is a column with the fix-ended foundation, and the right figure shows a column supported on a soft foundation. This also explains why softer foundations produced larger displacements in both directions under pushover loadings.

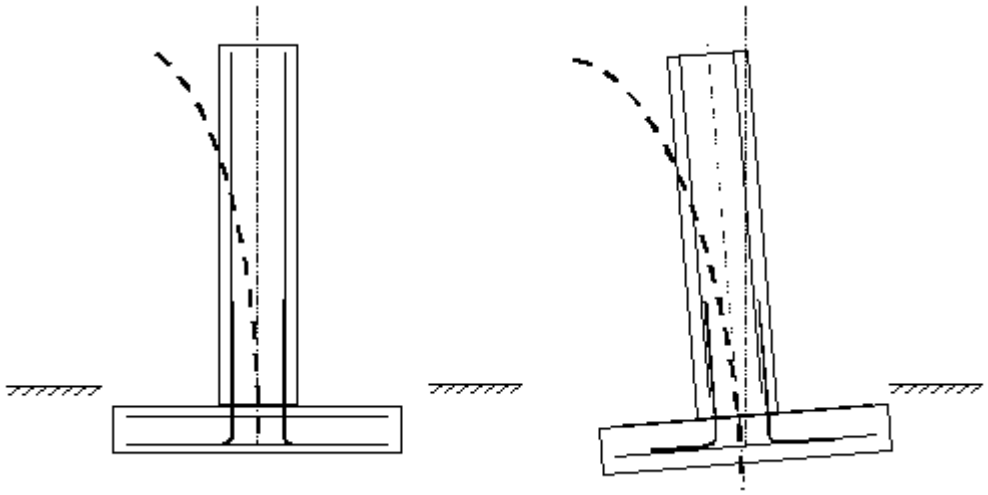

Figure 30 Deflection of columns supported by different footing boundary conditions.

Even though the absolute displacement at the top of the columns increased, the relative rotation of the column in reference to its end was reduced due to the shift of the yielding. It can be seen in Table 8 that both in longitudinal and transverse direction, the greatest performance ductility occurred in the case of fixed ended, in which the absolute displacement capacity were the least. It is very important that the variation in displacement capacity within different cases was much smaller than that in the force demand. Softer foundations reduced the input of forces to the superstructure and piers. Comparing the force demand at the performance point between the baseline case and the soft foundation case, both of which were in a realistic range, the demand was reduced by 25%.

Values of yielding displacement, Δ_{yield}, maximum displacement, $\Delta_{\max}$, performance displacement, $\Delta_{performance}$, displacement ductility, μ_{Δ}, and performance ductility, $\mu_{performance}$, of different cases are shown Table 8.

Table 8 Comparison of structure displacement and ductility with varying foundation stiffness

Dry Wash Bridge	Δ_{yield} (in.)	Δ_{max} (in.)	μ_{Δ}	Performance point			
				$\Delta_{performance}$ (in)	$\mu_{performance}$	Force demand (kips)	Demand variation from the Baseline
Longitudinal direction							
Baseline bridge	1.38	5.24	3.80	2.17	2.41	5586	0%
Fixed Ended	1.05	4.81	4.58	1.76	2.73	5852	5%
Soft Foundation	1.43	6.04	4.22	2.45	2.47	4121	-26%
Pinned End	2.09	6.60	3.16	2.64	2.50	3628	-35%
Transverse direction							
Baseline bridge	1.53	5.00	3.27	2.26	2.21	5226	0%
Fixed Ended	0.95	4.77	5.02	1.87	2.55	5321	2%
Soft Foundation	1.88	5.98	3.18	3.01	1.99	4029	-23%
Pinned End	1.85	6.10	3.30	3.23	1.89	3107	-41%

The transverse responses were more sensitive to the variation of foundation stiffness than the longitudinal response. This is because that column boundary conditions affected the frame effect at each bent, and the transverse reaction of the bridge relied primarily upon the bent frame effect, while longitudinally the abutment boundary conditions had larger influence on the bridge.

As noted previously, the yield and maximum displacements varied with different foundation properties. It was also observed that the performance point varied under different foundation circumstances, and the performance ductility tended to be larger as the foundations became stiffer. This is because as the maximum displacements of the softer foundation models were increased, their performance demands were raised at same time. But the increases were on proportional. Therefore, the performance ductility taken as the ratio of ultimate displacement over the performance displacement is not necessarily increased. In actuality, the performance ductility of a rigid foundation model is higher than those of softer foundation models.

For this particular bridge, the difference in performance ductility between the baseline model and fixed end model was rather small comparing to the force reduction. Hence more credit should be given to softer foundations. The presumption for a soft

foundation to be allowed is that the abutments are strong enough to tolerate large displacements and passive soil pressure associated with the joint movement. In addition, the superstructure should be continuous to avoid joints unseating.

The three cases investigated covered the possible foundations stiffness range for this bridge. The effect of different foundation stiffness on the longitudinal displacement of the bridge is noticeable but not significant. Transversely the influence was greater, and the displacement of flexible footings models was larger than that of rigid footing models. Nevertheless, the structure performance ductility did not necessarily increase as flexible foundations were employed, because the displacement demand may rise at same time. On the other hand, it is very evident that the force demand on the structure was greatly reduced by producing flexible footing supports in both transverse and longitudinal directions. To conclude, for the Dry Wash Bridge, as the performance ductility of the structure remains almost the same, a retrofitting method to create flexible soil-foundation interaction relationship is recommended to reduce the force demand. For other bridges analysis should be performed to estimate the "trade-off" of ductility and force demand reduction.

ABUTMENT STIFFNESS PARAMETRIC STUDY

Similar concerns about locking the connections between foundations and soil are given to abutments. As illustrated in section 2.1.3, the abutment retrofitting actions involve in stiffening or softening the interaction relationship between the abutments and the soil. It is simulated in the bridge model with a nonlinear link spring. The parametric study is based on the force-displacement relationship between the soil and the abutment by varying the stiffness of the nonlinear link spring.

Abutment Longitudinal Stiffness Sensitivity Study

As stated above, the behavior of the abutment link spring was estimated as nonlinear and was simulated with a trilinear force-displacement (F-d) relationship this research. The longitudinal nonlinear link spring was assigned with different force-displacement relationships to create three cases in the parametric study. Figure 31 shows the three link properties and the baseline trilinear relationship, in which K_o is the baseline initial stiffness. The three test cases are half, twice and four times of the initial baseline stiffness, shown as $1/2\ K_o$, $2K_o$, and $4K_o$ respectively in Figure 31.

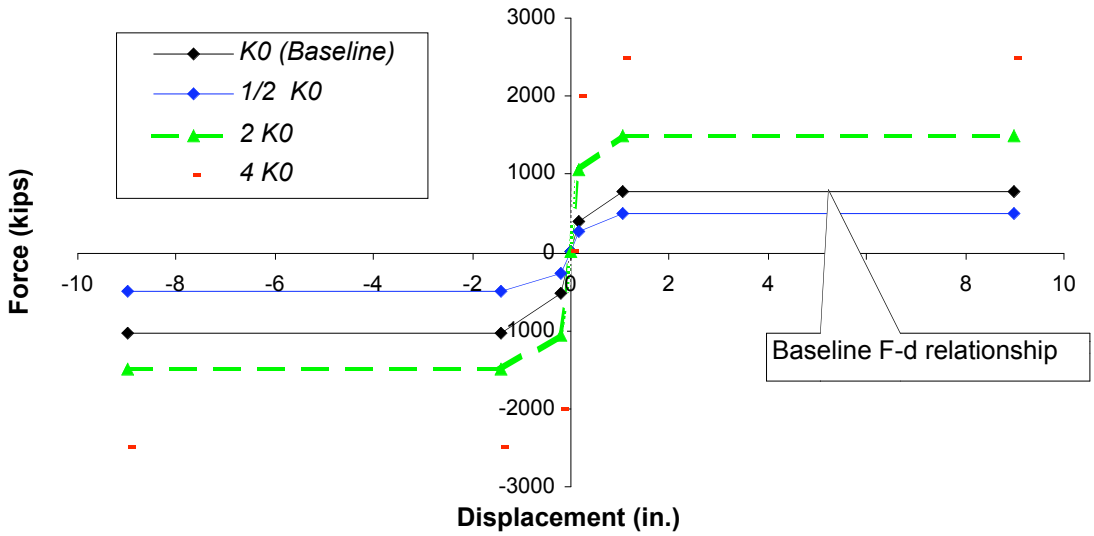

Figure 31 Force-Displacement relationship of three longitudinal abutment links

Responses of different cases are compared with the baseline pushover curve shown in Figure 32. As expected, stiffer longitudinal abutment springs increased the stiffness of the whole structure in the same direction, and in the transverse direction the stiffness and responses with variable longitudinal links were almost identical as shown in Figure 33.

It has been observed that when the longitudinal stiffness of the abutment was doubly enlarged, the stiffness of the whole structure increased only 11%; and when the stiffness was four times larger, the structure was 48 % stiffer. The maximum displacements obtained in the three cases varied within a range of 5% of the original response, which is almost negligible.

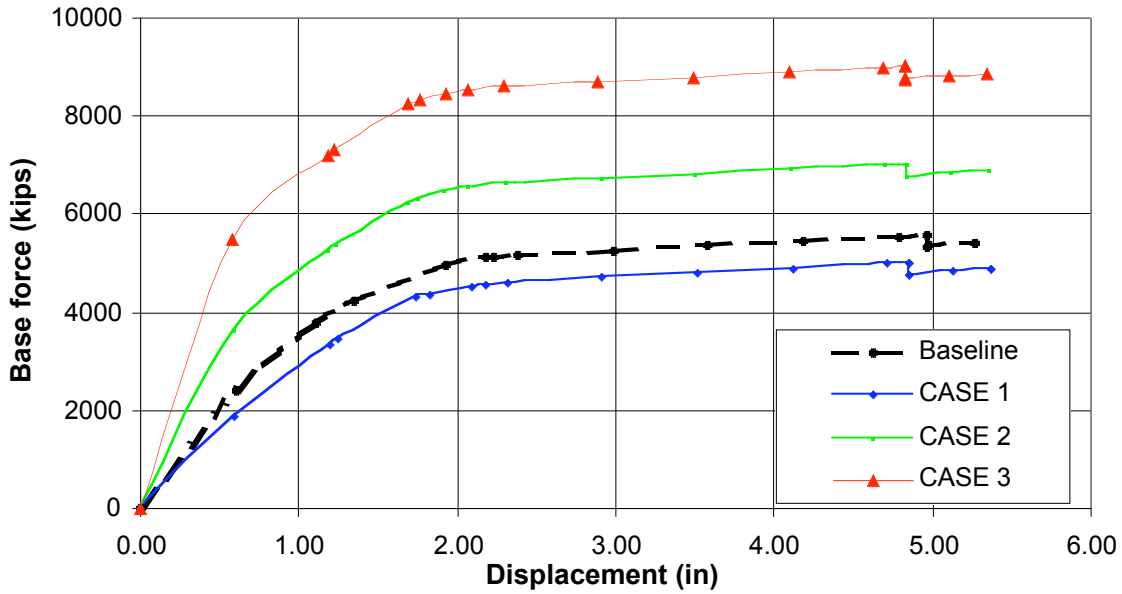

Figure 32 Longitudinal pushover curves of models with different longitudinal abutment stiffness

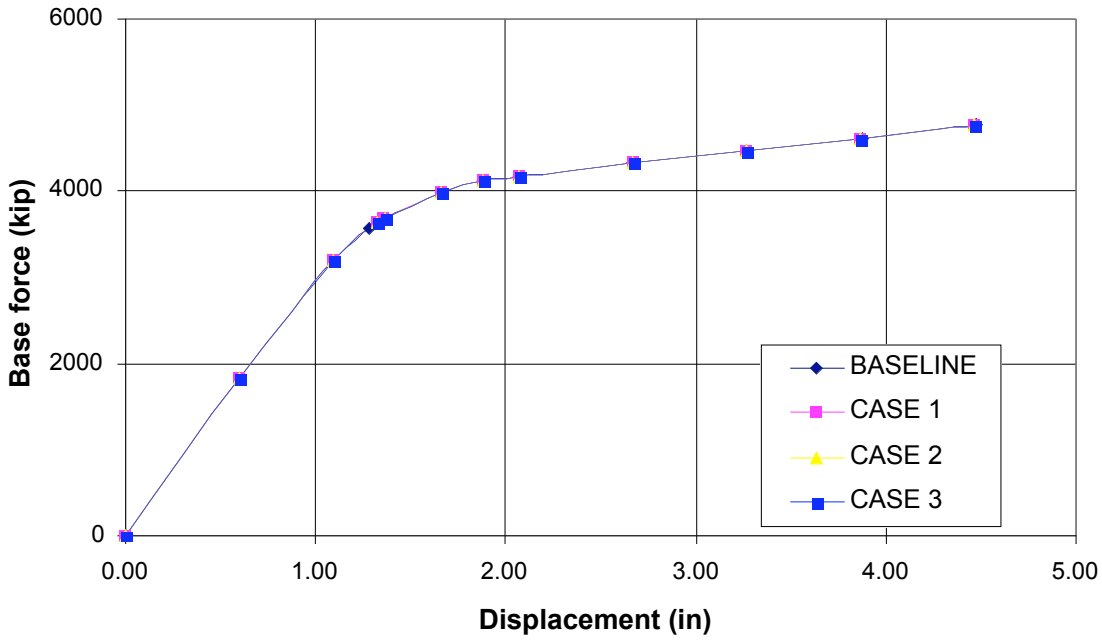

Figure 33 Transverse pushover curves of models with different longitudinal abutment stiffness

Table 9 shows the values of displacements and ductility of different cases. The displacement ductility, μ_Δ, of the structures showed little variation, since the yielding

displacement, Δ_{yield}, and maximum displacement, $\Delta_{\max}$, for all cases were very close. The sequence of plastic hinge formation did not change due to different spring properties. This indicated that the varying abutment stiffness increased the structure stiffness without altering the deflection and failure mode of the structure.

Table 9 Comparison of structure displacements and stiffness change with varying longitudinal abutment stiffness

Varying Longitudinal links	Δ_{yield} (in.)	$\Delta_{\max}$ (in)	μ_{Δ}	$\frac{\text{Response stiffness}}{\text{Baseline stiffness}}$	$\Delta_{performance}$ (in)	$\mu_{performance}$
Original Link	1.11	5.27	4.75	100%	2.086	2.53
Case One ($0.5K_0$)	1.19	5.37	4.51	80%	2.313	2.32
Case Two ($2K_0$)	1.23	5.30	4.31	125%	1.744	3.04
Case Three ($4K_0$)	1.22	5.35	4.39	183%	1.376	3.89

It can be seen from Table 9 that the performance ductility increased as the abutments were stiffened. This is due to the same reason related to the capacity spectrum shape that explained in section 5.4. for foundations boundary conditions. The change in performance ductility is trivial when comparing to the associated force demand change. It is recommend that retrofitting application that stiffens the locking connection between abutments and the backwall for this type of bridge be avoided.

Abutment Transverse Stiffness Sensitivity Study

Similar to longitudinal abutment springs, three cases were created by varying the transverse abutment spring stiffness. Their force-displacement relationship curves are shown in Figure 34, in which K_{to} is the transverse baseline initial stiffness. The three test cases are half, twice and four times of the initial baseline stiffness, shown as $1/2\ K_{to}$, $2\ K_{to}$, and $4\ K_{to}$ respectively.

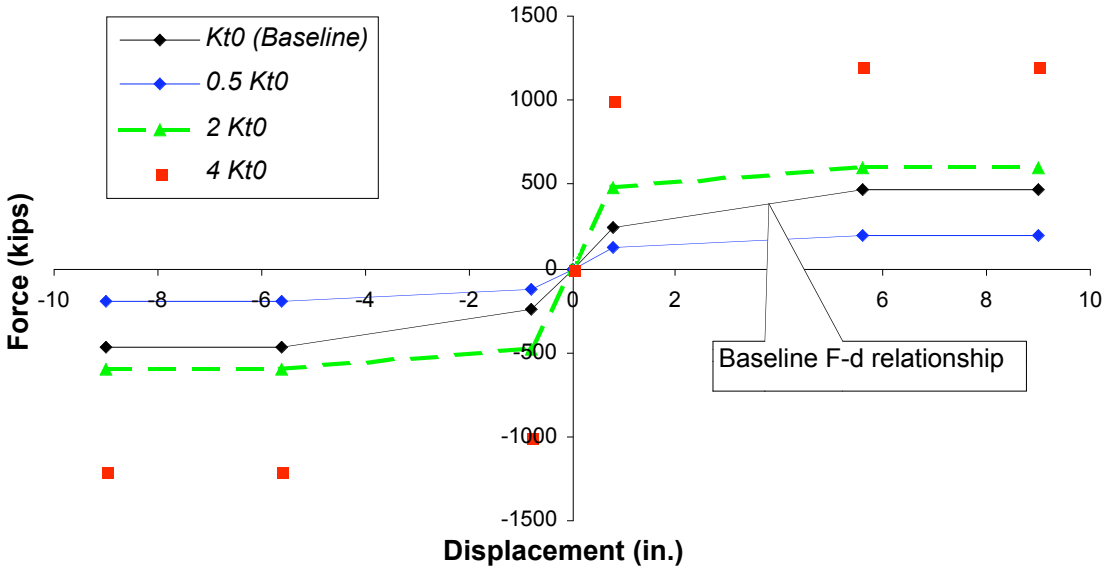

Figure 34 Force-Displacement relationship of three transverse abutment links

Case 1 and Case 2 defined the upper and lower bound of possible stiffness range of the transverse abutment. Case 3 simulated a very stiff response of the abutment. The pushover curves for the transverse direction are compared in Figure 35. Similar comparison is made in Figure 36 for the longitudinal direction pushover.

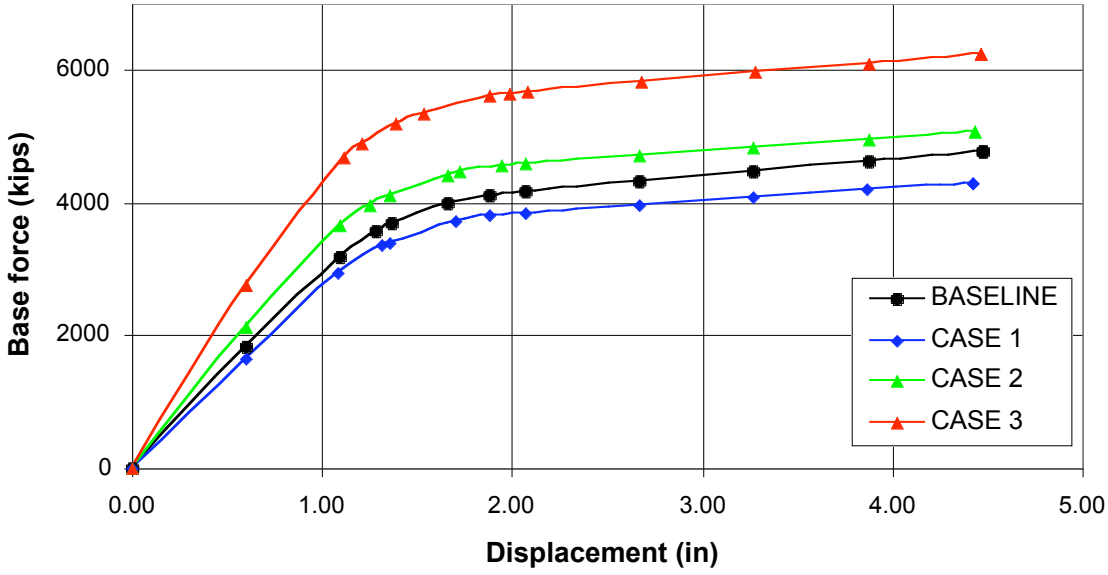

Figure 35 Transverse pushover curves of varying transverse link models

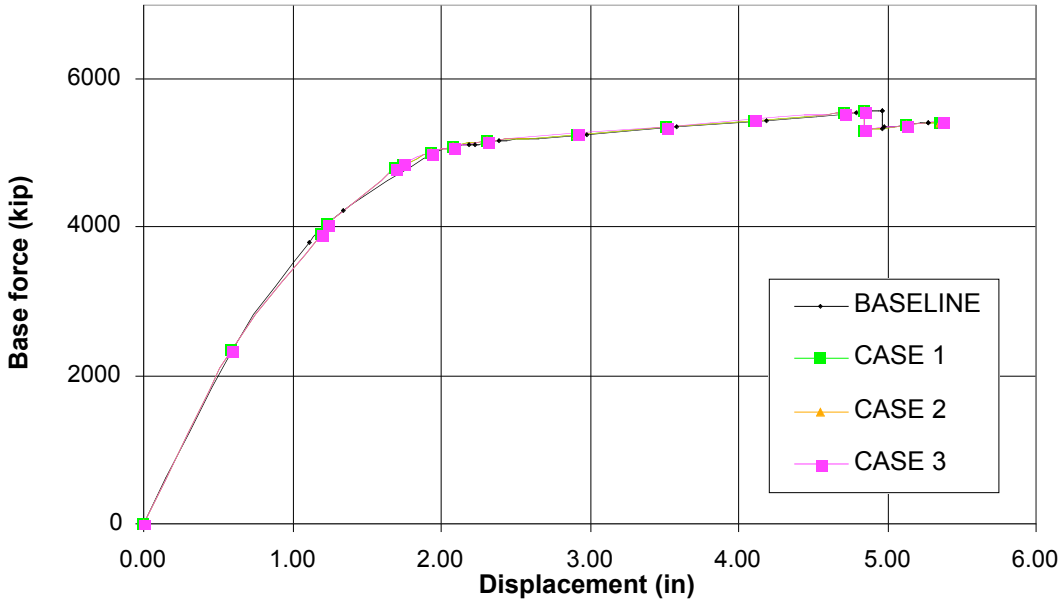

Figure 36 Longitudinal pushover curves of varying transverse link models

For the transverse direction, the bridge response was less sensitive to the variation of transverse abutment stiffness. This is due to the abutment not being the major supply of transverse resistance of the bridge. The transverse stiffness of the bridge was more relied upon columns and framing effect of piers. This was verified in section 5.4, as the transverse responses were more sensitive than the longitudinal responses to the stiffness of the foundations.

Table 10 Comparison of structure displacements and stiffness change with varying transverse abutment stiffness

Varying Longitudinal links	Δ_{yield} (in.)	Δ_{max} (in)	μ_{Δ}	Stiffness variation vs. baseline	$\Delta_{performance}$ (in)	$\mu_{performance}$
Original Link	1.09	4.47	4.10	100%	2.187	2.04
Case 1 ($0.5K_0$)	1.08	4.43	4.10	75%	2.170	2.04
Case 2 ($2K_0$)	1.10	4.43	4.03	111%	2.174	2.04
Case 3 ($4K_0$)	1.11	4.47	4.03	148%	2.176	2.05

The corresponding response stiffness change was still considerably large, which indicated that the force demands differed greatly between various cases. The variation of the maximum displacement on transverse direction was less than 2.8%. However, various transverse stiffness of the abutments produced very close performance ductility for this bridge, so force demand would need more careful consideration.

As a conclusion, retrofitting bridge abutment aimed at increasing the stiffness may result in little improvement son the global structure displacement capacity. It will induce a great increase of the force demand to the structure. Therefore, if not inevitable, retrofitting applications that increase the locking of the abutment and the soils are not recommended. A better option would be extending the effective seating length.

COLUMN RETROFIT PARAMETRIC STUDY

Column steel jacketing is the most popular retrofit method employed in bridge strengthening and retrofitting programs. It has been proven to be an effective method by both experimental and analytical research. Often, all columns of a bridge are jacketed to complete the retrofitting goal, however this may not be necessary. Retrofitting some critical columns may meet performance requirements with significant reduction in costs. In this section, eighteen scenarios were studied to compare the effects of different jacketing plans and their ability to enhance the ductility of a bridge system.

To facilitate the location of columns and hinges in the following discussion, the columns were labeled as shown in Figure 37. For example, column labeled as "1B" was at Bent 1 in row B, and the hinge at the top of column "1B" was named as "1B1", while the bottom hinge was labeled as "1B2".

Figure 38 and Figure 39 represent pushover curves for six of the eighteen cases as compared to the baseline pushover curve. Note that the stiffness enhancement by steel jacketing was ignored in this research. The pushover curves followed the same path as that of the baseline, but extended the maximum displacements. This means that the failures were postponed by better ductility of columns. The yielding in the different cases occurred at the same point, for the reason that the yielding of the column sections remaining unchanged after the columns were steel jacketed. But the rotation capacity of hinges was greatly enhanced due to the added confinement provided by steel jacketing, which resulted in better ductility.

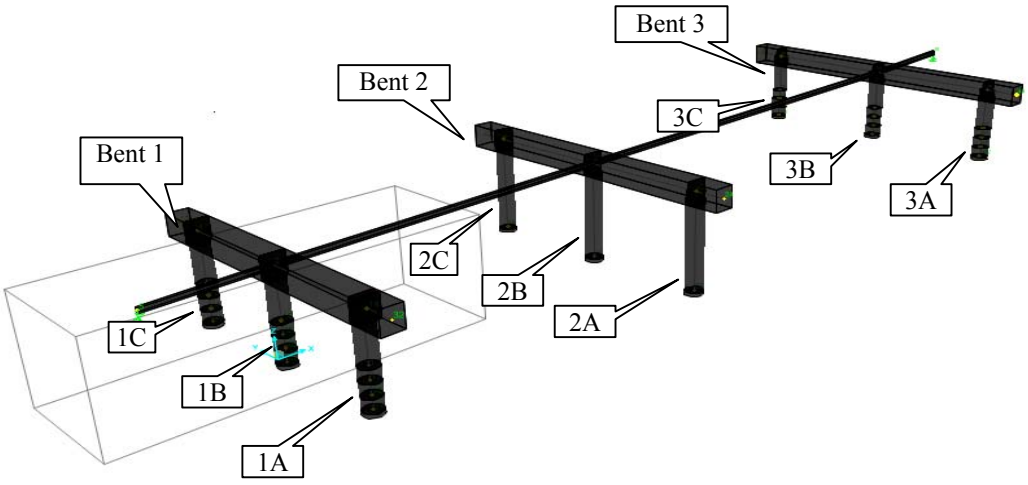

Figure 37 Labeling of columns and Bents

The generation of the demand spectrum assumed an energy-consuming path in the shape of the capacity spectrum, below which the area is the energy consumed. Because all the curves were in the same shape, the single demand spectrum remained the same for different cases. Hence, for all the cases, the performance point is (2.086 in, 5053kip) on the longitudinal curves and (2.187in, 4205kip) on the transverse pushover curves. Therefore, the ultimate displacement became the only variable in the responses, and can be used as the reference to evaluate the structure ductility. Table 11 shows the maximum displacements of the structure after different column jacketing plans were complemented.

The shear capacity the existing columns have been checked and demonstrate sufficient shear strength to sustain the pushover procedure. So in this research the shear demand reduction on unretrofitted columns due to selective column jacketing was not considered. Moreover, the displacement demands on the structure are not changed by column stiffness. Therefore, the stiffness enhancement of columns by steel jacketing was not considered in this research.

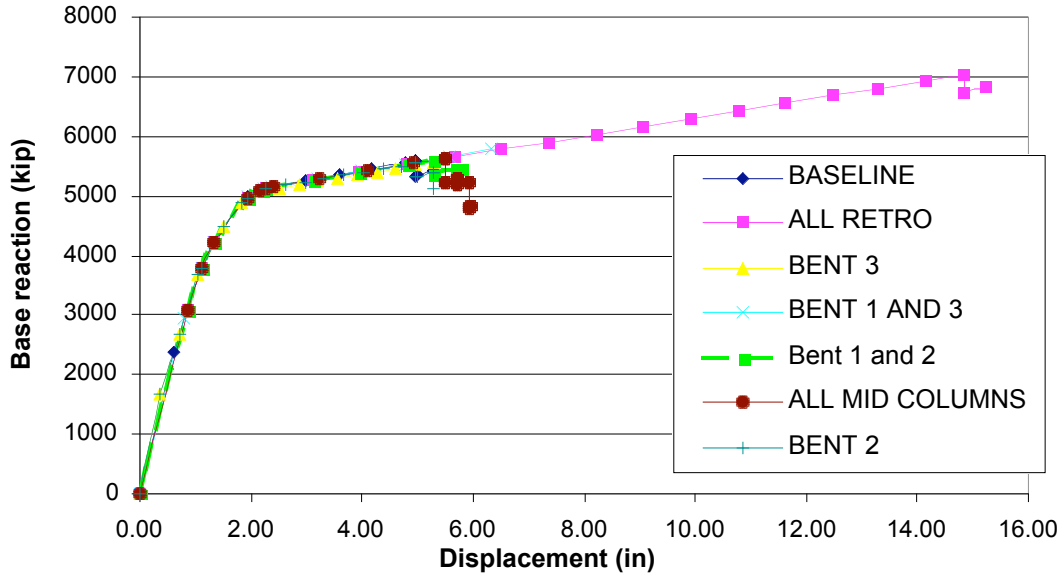

Figure 38 Longitudinal pushover curves of different column retrofitting plans

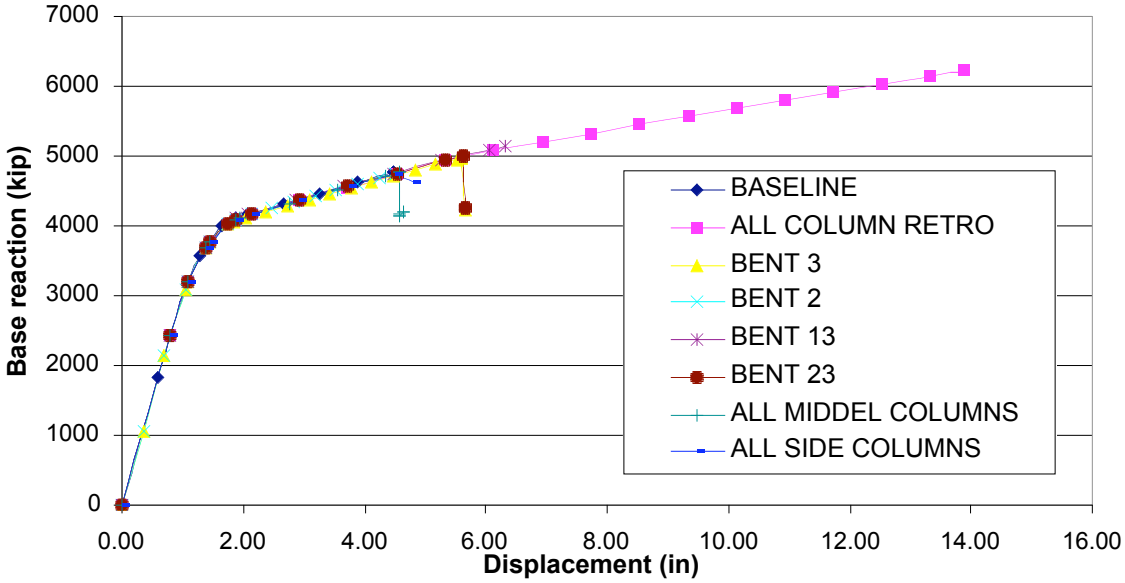

Figure 39 Transverse pushover curves of different column retrofitting plans

Table 11 Comparison of structure maximum displacements of different retrofitting plans

Comparison of structure maximum displacement of different retrofitting plans					
Plans		Longitudinal pushover		Transverse pushover	
CASES	Retrofitting plan configuration	Δ_{max} (in)	Increase ratio over baseline	Δ_{max} (in)	Increase ratio over baseline
Baseline displacement		5.24 in.		5.00 in.	
GROUP 1: THREE COLUMNS RETROFITTED					
CASE 1		5.87	12.02%	5.93	**18.60**%
CASE 2		5.25	0.19%	5.14	2.80%
CASE 3		6.01	**14.69%**	5.23	4.60%
CASE 4	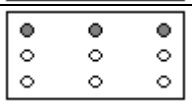	5.25	0.19%	5.22	4.40%
CASE 5	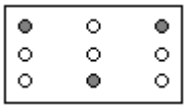	5.25	0.19%	5.23	4.60%
GROUP 2: FOUR COLUMNS RETROFITTED					
CASE 6	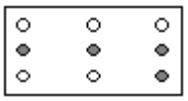	6.02	14.89%	5.24	4.80%
CASE 7	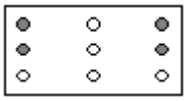	6.02	14.89%	5.55	11.00%
CASE 8	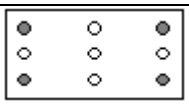	5.25	0.19%	5.46	9.20%
CASE 9	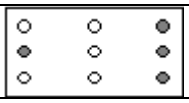	6.02	14.89%	6.01	**20.20%**
GROUP 3: FIVE COLUMNS RETROFITTED					
CASE 10		6.63	**26.53%**	6.31	26.20%
CASE 11	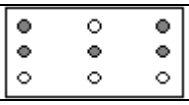	6.02	14.89%	5.55	11.00%

CASE 12	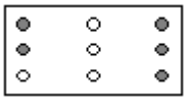	6.63	**26.53%**	6.33	**26.60%**
GROUP 4: SIX COLUMNS RETROFITTED					
CASE 13	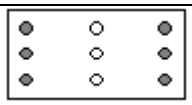	7.11	**35.69%**	6.95	**39.00%**
CASE 14		5.88	12.21%	5.93	18.60%
CASE 15		5.25	0.19%	5.47	9.40%
CASE 16	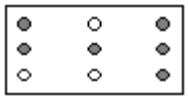	6.63	26.53%	6.78	35.60%
GROUP 5: SEVEN COLUMNS RETROFITTED					
CASE 17	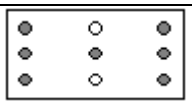	7.84	49.62%	6.95	39.00%
GROUP 6: ALL COLUMNS RETROFITTED					
CASE 18		15.22	190.46%	14.36	187.20%

In the above table, the plans were compared in groups that associated with the number of columns that were jacketed. Increase ratios that are the greatest in each group were highlighted. Case 18 was to steel jacket all the columns. It can be seen that the enhancement of the displacement of the structure was very significant, which was about 190% for the longitudinal direction and 210% for the transverse direction. Results from other combinations were much less than Case 18. Case 17 retrofitted seven out of nine columns, however, the increase was 32.8% for the longitudinal direction and 40.9% for the transverse direction. The two unjacketed columns failure caused the structure collapse. This indicated that the displacement demands to the unjacketed columns was not reduced, even though the full structure ductility was enhanced after critical columns jacketed. Nevertheless, the applications of partially column retrofitting plans produced satisfactory results to meet the performance requirement.

In the first group that three columns were to be jacketed, Case 3 presented the best structure ductility enhancement of 13% for the longitudinal direction when compared to other three columns retrofitting plans. In contrast, Cases 4, 5, 8 and 15, where no middle columns were retrofitted, the longitudinal displacement was increased by 0.1%.

For the transverse direction, Case 1 that was to jacket the three columns at Bent 3 increased ductility by 26.5%, which was much higher than those of other plans in group 1. The main reason is that the columns at Bent 3 were a little shorter than the columns at other bents. As explained in modal analysis, the superstructure of the bridge was very stiff and tended to move as a unit. Hence the variation of the deflections of nodes on the superstructure was very small. Larger rotation demand estimated as a drift ratio was applied to shorter columns, but the curvature ductility was the same for all column sections. Hence shorter columns were more vulnerable to displacement demand.

Comparing the results from the eighteen cases, conclusions can be drawn. To better improve the bridge longitudinal ductility, more credit should be given to retrofitting plans that involves jacketing of the middle columns and columns with less effective height. For the transverse direction, priority should be given to shorter columns since they are more vulnerable under higher rotation demand. It is the effective height rather than the physical height of the column that is used to estimate the vulnerability. The effective height of a column could be altered by its boundary conditions. For example, a deep embedded column can be regarded as a pile shaft extending into the ground, and an inground plastic hinge may occur in the soil according to the moment distribution. The effective height of the column taken as from the top of the column to the plastic hinge location plus the length of tensile strain penetration is thus reduced. Retrofitting method exist to isolate the surrounding soils from the columns so that the effective height is increase and a more flexible boundary condition is created.

For the Dry Wash Bridge, as discussed in baseline results analysis, the longitudinal ductility was better than the transverse ductility. So retrofitting plans that are more effective in enhancing the transverse performance are more favorable. Considering the cost and the performance, plans of Case 9, and Case 16 are favorable in retrofitting the Dry Wash Bridge.

CONCLUSIONS

The results from this study indicate that retrofit strategies of reinforced concrete bridges can be optimized to achieve the performance goals of a given structure. As a result, considerable economic savings can be realized in retrofitting applications. Short spanned reinforced concrete bridges show that in translational vibration the greatest mass participation ratios are usually associated with the fundamental vibration modes. The superstructure tends to move as a unit both in longitudinal and transverse directions, and the influence of higher vibration modes is negligible. Bridge abutment rotational constraints do not have much influence on the deflection of the superstructure for these type of bridge.

Retrofitting applications on bridge footings can stiffen or soften the connection between the footing and soils. Bridges supported by softer foundations can tolerate larger displacements, however, due to the change in the seismic demand, the performance ductility varies but not necessarily increasing as the foundations are softened. That is due to the increases in the maximum and performance displacements not necessarily being proportional. It has been found that for the longitudinal direction, the varying stiffness produced a variation in the lateral displacement of 20%, but the longitudinal ductility range was less than 10%. For the transverse direction, the variation in displacements was within 12% and the ductility values remained close. Force input to the structure can vary greatly due to the change in the foundation properties, especially in the transverse direction. By softening the baseline foundation properties to a practical level, the shear reaction of the structure could be reduced by 25%, while its displacement change was less than 10%. Therefore, the overall change in the displacement due to the presence of varying foundation stiffness is minimal compared to the force demand reduction caused by softer foundations. A flexible foundation connection is recommended for this type of bridge to reduce the force demand, as the ductility of the structure remains almost the same. For other types of bridges, analysis should be performed to estimate the "trade-off" of ductility and force demand reduction.

The transverse response of a bridge relies more on the framing effect of piers than single column and abutments, so foundation properties tend to have a larger influence. In contrast, variable abutment properties have larger influence on the longitudinal stiffness than on the transverse stiffness of the structure. For both directions, the displacement variation associated with abutment stiffness change is very small. Therefore, retrofit techniques for bridge abutment aimed at increasing the stiffness may result in little improvement on the global structure displacement capacity. They will, however, induce a

great force demand on the structure. For this type of bridges, retrofitting applications that increase the locking of the abutment and the soils should be avoided.

Steel jacketing presents the best approach to improve the bridge ductility. By comparing results from eighteen analysis cases, it is concluded that middle columns and columns with shorter effective height are the most critical for improving the bridge longitudinal ductility. For the transverse direction, priority in retrofitting should be given to shorter columns because similar displacements at the top of the columns indicate larger drift ratios. It should be noted that it is the effective height rather than the physical height of the column that is used to estimate the vulnerability. The effective height of a column can be changed by changing its boundary conditions. A deep embedded column that allows an inground plastic hinge to occur can be retrofitted by elongating their effective length. The column would rotate around the plastic hinge rather than the end of the column. Retrofitting methods exist to isolate the surrounding soils from the columns so that the effective height is increase and a more flexible boundary condition is created.

Analytical research may be conducted to better understand the performance of a bridge prior to the implementation of retrofitting plans. Bridges may perform well in one direction, while exhibiting poor response in the other direction. The Dry Wash Bridge has better ductility in the longitudinal direction, so the retrofitting plans should be more focused in the transverse direction.

By attaching more importance to the columns with shorter effective lengths and as well as the middle columns, two column combination plans were recommended to retrofit the Dry Wash Bridge. One is to jacket the three columns at the right edge bent and the middle column at the left edge bent. The longitudinal and transverse displacement capacities can increase by 13.6% and 28.5% respectively. The other is to jacket six columns, which consist of three columns at the left edge bent, the middle column at center bent, and the two columns at the right edge bent. This plan can produce 21.6% and 42.5% increase in the longitudinal and transverse displacements respectively.

ACKNOWLEDGMENTS

This research was conducted under the sponsorship of the Washington State Department of Transportation contract number T2696-02 in cooperation with the Federal Highway Administration (FHWA). Their support is greatly appreciated as it enabled the researchers to pursue in-depth studies on the performance of retrofitted bridges.

I am sincerely grateful to my committee members Dr. Rafik Itani for his guidance and insightful instructions to my research work, Dr. David G. Pollock for reviewing and providing insight on the thesis, and Dr. Cole C. McDaniel for his patient assistance and guidance throughout the project. Appreciation is extended to the civil engineering faculty and staff at Washington State University for their assistance and guidance throughout my two-year graduate studies. I would like to express my gratitude to my fellow graduate students and friends for their encouragement and support.

Most of all, my sincere thanks and appreciation go to my parents, Li and Weimin, for their love, devotion and belief in me and for their continued support throughout the years of my academic career.

REFERENCES

Abeysinghe, R. S., Gavaise, E., and Rosignoli, M. (2002). "Pushover analysis of inelastic seismic behavior of Greveniotikos Bridge." *Journal of Bridge Engineering*, ASCE, Vol. 7, No. 2, Mar./Apr., pp.115-126.

Aboutaha, R. S., Engelhardt, M. D., Jirsa, J. O. (1999). "Rehabilitation of shear critical concrete columns by use of rectangular steel jackets." *ACI Structural Journal*, Vol. 96, No.1, Jan./Feb., pp. 68-78.

ACI-318 (1999). "Building Code Requirement for Structural Concrete." American Concrete Institute, Detroit, Michigan

Applied Technology Council (ATC). (1996). "Seismic Evaluation and Retrofit of Concrete Bridges." *ATC-40*, Redwood City, California

Biddah, A., Ghobarah, A., and Aziz, T. S. (1997). "Upgrading of nonductile reinforced concrete frame connections." *Journal of Structural Engineering*, ASCE, Vol. 123, pp. 1001-1010.

Bowles, Joseph E. (1988). *Foundation Analysis and Design.* McGraw-Hill Book Company, New York

Caltrans. Seismic Design Criteria 1.1. (1999). California Department of Transportation.

Chai, Y. H., Priestley, M. J. N., Seible, F. (1994). "Analytical model for steel-jacketed RC circular bridge columns." *Journal of Structural Engineering*, Vol. 120, pp. 2358-2376.

Cofer, W. F., McLean, D. I., and Zhang, Yi. (1997). *Analytical Evaluation of Retrofit Strategies for Multi-Column Bridges*. Technical report, Washington State Transportation Center, Department of Civil and Environmental Engineering, Washington State University.

Cooper, J.D., Friedland, I. M., Buckle, I. G., Nimis, R. B., and Bobb, N. M. (1994). "The Northridge Earthquake: Progress Made, Lessons Learned in Seismic Resistant Bridge Design." *Public Road*, Vol. 58. No. 1., pp. 26-36

Daudey, Xavier, and Filiatrault, Andre. (2000). "Seismic evaluation and retrofit with steel jackets of reinforced concrete bridge piers detailed with lap-splices." *Canadian Journal of Civil Engineering*, Vol. 27, No. 1, pp. 1-16.

Federal Emergency Management Agency, (1997). *National Earthquake Hazards Reduction Program (NEHRP) Commentary on the Guidelines for the Seismic Rehabilitation of Buildings (FEMA 274).* Washington, D.C.

Federal Emergency Management Agency, (1997). *National Earthquake Hazards Reduction Program (NEHRP) Guidelines for the Seismic Rehabilitation of Buildings (FEMA 273).* Washington, D.C.

Federal Emergency Management Agency, (2000). *Prestandard and Commentary for the Seismic Rehabilitation of Buildings (FEMA 356).* Washington, D.C.

Ghasemi, H., Otsuka, H., Cooper, J. D. and Nakajima, H. (1996). "Aftermath of the Kobe Earthquake." *Public Road*, Vol. 60. No. 2.

Ghobarah, A., Aziz, T. S., Biddah, A. (1997). "Rehabilitation of reinforced concrete frame connections using corrugated steel jacketing." *ACI Structural Journal*, Vol. 94, pp. 283-294.

Hsu, Y. T. and Fu, C. C. (2000). "Study of Damaged Wushi Bridge in Taiwan 921 Earthquake.", *Practice Periodical on Structural Design & Construction*, ASCE Vol. 5, No. 4, pp. 166-171, Nov. 2000

International Code Council (ICC) (2000). *International Building Code*, Falls Church, Virginia

Kutter, B. L., Martin, G., Hutchinson, T., Harden, C., Gajan, S., and Phalen, J. (2003). "Study of Modeling of Nonlinear Cyclic Load-Deformation Behavior of Shallow Foundations." Status report, PEER workshop, March, 5, 2003, Berkeley, California

Mackie, Kevin and Stojadinovic, B. (2002). "Bridge Abutment Model Sensitivity for Probabilistic Seismic Demand Evaluation", *3rd National Seismic Conference& Workshop on Bridges and Highways*, April 28-May 1 2002, Portland, Oregon

McLean, D. I. and Marsh, M. L. (1999). "Seismic Retrofitting of Bridge Foundations." *ACI Structural Journal*, Vol. 96, pp. 174-182.

Naito, C. J., Moehle, J. P. and Mosalam, K. M. (1999). "Evaluation of Bridge Beam-Column Joints Under Simulated Seismic Loading." *ACI Structural Journal*, Vol. 96, pp. 519-532.

Paulay T. and Priestley, M. J. N. (1992). *Seismic Design of Reinforced Concrete and Masonry Buildings*. John Wiley & Sons, Inc., New York.

Priestley, M. J., Seible, F., and Calvi, G. M. (1996). *Seismic Design and Retrofit of Bridges*. John Wiley & Sons, Inc., New York

Priestley, M. J., Seible, F., Xiao, Y. (1994). "Steel jacket retrofitting of reinforced concrete bridge columns for enhanced shear strength; theoretical considerations and test design." *ACI Structural Journal*, Vol. 91, pp. 394-405.

Priestley, M. J., Seible, F., Xiao, Y. (1994). "Steel jacket retrofitting of reinforced concrete bridge columns for enhanced shear strength; test results and comparison with theory." *ACI Structural Journal*, Vol. 91, p. 537-551.

Ranf, T. R., Eberhard, M. O., and Berry, M. P. (2001). "Damage to Bridges During the 2001 Nisqually Earthquake." PEER, Nov. 2001, Berkeley, California

SAP2000 8.0.8 Structural Analysis Program (2000). Computer and Structures, Inc. Berkeley, California

Xiao, Y., Priestley, M. J. and Seible, F. (1996). "Seismic Assessment and Retrofit of Bridge Column Footings." *ACI Structural Journal*, Vol. 93, pp. 79-94.

XTRACT v.2.6.2 Educational, Cross Section Analysis Program (2002), Imbsen and Associates, Inc., Sacramento, California

Zhang, Yi, Cofer, W. F., McLean, D. I. (1999), "Analytical evaluation of retrofit strategies for multicolumn bridges." *Journal of Bridge Engineering,* ASCE, Vol. 5, No. 2, May, pp.143-150.

APPENDIX

STRUCTURAL MODEL CHARACTERIZATIONS OF DRY WASH BRIDGE

1) Foundation spring stiffness constants

An average dimension of 15 by 16 feet^2 for rectangular footing was calculated for foundation spring stiffness constants. The modulus of elasticity of the soil was approximated as 1000 ksf, so the shear modulus G=2.57 ksi, in which Poisson's ratio, ☒, is taken as 0.35. Shape factor, α, and embedment factor, β that were used to adjust the spring stiffness are in Appendix. Table 1 shows the values of spring constants used in the model for all column footings.

Values of spring coefficients used in Dry Wash model

Linear spring stiffness (k/in)	k_x	k_y	k_z
	2655	2297	2144
Rotational spring stiffness (k/rad)	k_{rx}	k_{ry}	☒
	30702159	22802885	31162520

2) Abutment spring stiffness constants

The abutment was about 89 feet wide; the depth that engaged fully in the compression direction was about 2 feet and 1.5 feet in the longitudinal direction.

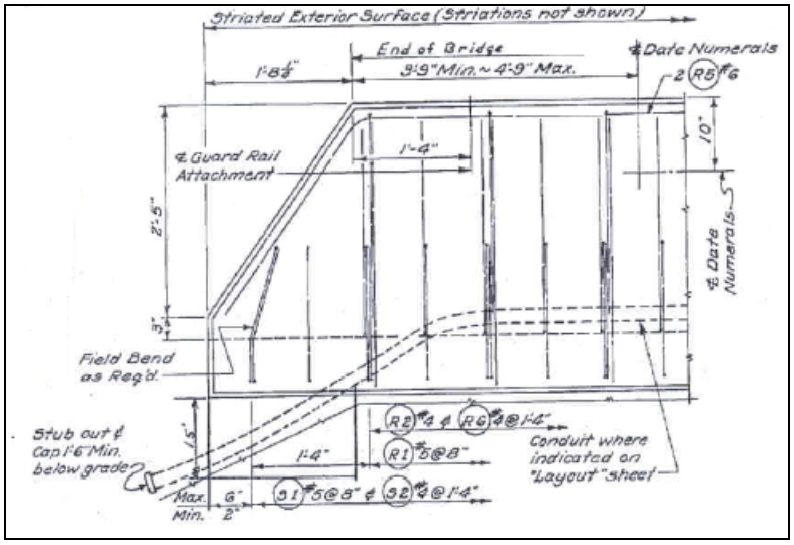

Detailing of the abutment of Dry Wash Bridge

According to the chart of the experimental results from UC-Davis study, the longitudinal springs of the abutment, which was modeled with multi-linear elastic link elements, followed a force-displacement relationship as the following figure in solid line.

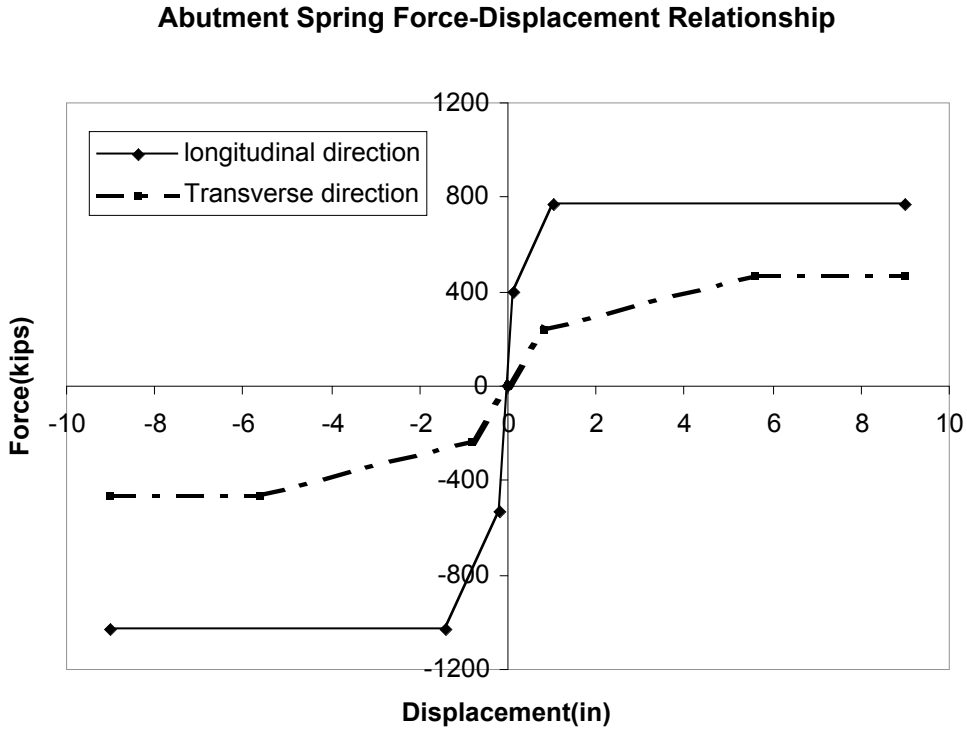

Abutment lateral force-displacement relationship

On the transverse direction, deeper wingwalls were constructed that the depth that engaged in transverse movement was estimated as 8 feet. The transverse abutment spring force-displacement relationship is shown as dashed line in the above figure.

The vertical spring stiffness and rotational spring constants were difficult to determine due to the insufficiency of the soil property information. The equivalent circular footing method was employed again. Two extreme cases were studied that are free of rotation and fixed of rotation. Results of these two cases shown in section 4.2.1 proved to be close enough to ignore the effect of rotational spring stiffness. Hence, abutment springs are modeled as free of rotation.

3) Plastic hinge characterization

The tensile strain of longitudinal yielding penetrated with a length of:

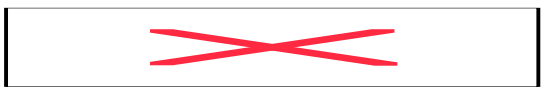

.

The superstructure and foundations of the bridge were both very stiff, so columns were under double bending under lateral loading. To evaluate the location of the contraflexure points, plastic hinges were reasonably approximated to be at the ends of effective columns at first. By applying lateral static forces on the bridge, the moment

diagram indicated that contraflexure points locate at the middle point of the effective columns. So "L" used to evaluate the plastic hinge length was taken as half of the effective column height. The effective column height in the Bent 2 is different from Bent 1 and Bent 3, because the boundary condition at the edge bents are foundations that are deep under soil. As a result, hinge of columns at edge bent tend to occur in a region close to the surface of the soil. The effective column height at edge bents were estimated as clear column height H_c plus strain penetration into cap beam and below soil. The embedment depths in bent 1 and 3 were very close and regarded as identical assuming that soil properties are same too.

Columns in Dry Wash are circular with a diameter of 60 inches reinforcing with 21 # 11 Grade 60 rebar under a cover concrete of 2 inches thick. So the plastic hinge length of columns in bent 2 of Dry Wash is:

$$L_p = 0.08L + 0.15 f_{ye} d_{bl} = 0.08 \times 170 + 0.15 \times 60 \times \frac{11}{8} = 25.975in$$

$$\geq 0.3 f_{ye} d_{bl} = 0.3 \times 60 \times \frac{11}{8} = 24.75in$$

In bent 1 and 3, column plastic hinge length would be:

$$L_p = 0.08 \times 130 + 0.15 \times 60 \times \frac{11}{8} = 22.775in$$

,

which is less than $0.3 f_{ye} d_{bl} = 0.3 \times 60 \times \frac{11}{8} = 24.75in$, so 24.75 inches would be used as the plastic hinge length in bent 1 and 3, over which curvature is assumed to be constant to evaluate the deflection of the columns.

The maximum compression strain is calculated as:

$$\rho_s = \frac{4A_{sp}}{D's} = \frac{4 \times 0.2}{56 \times 6} = 0.00238$$

$$\varepsilon_{cu} = 0.004 + \frac{1.4 \rho_s f_{yh} \varepsilon_{su}}{f'_{cc}} = 0.004 + \frac{1.4 \times 0.00238 \times 60 \times 0.1}{6.65} = 0.007$$

So, 0.007 will be used as the maximum compression strain, which is more than twice larger than the 0.003 strain used in design.

4) Design of retrofitting steel jacketing and characterization of retrofitted columns

Assuming that the maximum strain in core concrete is 0.02, the necessary thickness of the steel jacketing applied on the columns of Dry Wash would be calculated as below:

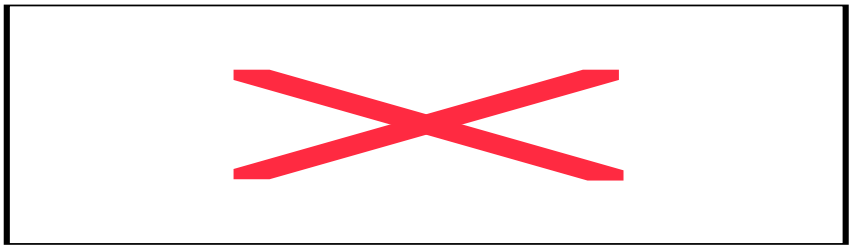

A steel jacket of 0.3-inch thickness was used outside of a one-inch thick concrete grout. Properties associated with this confinement were checked as following:

$$\rho_s = \frac{4t_j}{D} = \frac{4 \times 0.3}{60 + 2 \times (1 + 0.3)} = 0.02; \quad \frac{f_{yh}}{f_c^{'}} = 7.33$$

With the confining steel ratio and strength ratio above, the steel jacketing confined concrete strength can be calculated by its ratio over unconfined concrete strength from Figure 10: $\frac{f_{cc}^{'}}{f_c^{'}} = 1.5 \Rightarrow f_{cc}^{'} = 8ksi$, which is same as assumed.

The ultimate concrete compression strain for the steel jacketed circular column of Dry Wash Bridge is:

$$\varepsilon_{cu} = 0.004 + \frac{5.6 t_j f_{yj} \varepsilon_{sm}}{D f'_{cc}} = 0.004 + \frac{5.6 \times 0.3 \times 40 \times 0.15}{62.6 \times 8} = 0.024$$

For conservation, the ultimate concrete compression strain used in XTRACT for the calculation of the moment-curvature relationship is taken as 0.02, which is also the largest strain recommended by XTRACT.